

**FUNCTIONAL NEURONS FROM HUMAN BONE MARROW
DERIVED MESENCHYMAL STEM CELLS**

by
EDA KUŞ

**Submitted to the Graduate School of Engineering and Natural Sciences
in partial fulfilment of
the requirements for the degree of Master of Science**

**Sabancı University
Jul 2023**

EDA KUŞ 2023 ©

All Rights Reserved

ABSTRACT

FUNCTIONAL NEURONS FROM HUMAN BONE MARROW DERIVED MESENCHYMAL STEM CELLS

EDA KUŞ

Molecular Biology, Genetics and Bioengineering MS.c THESIS, JUL 2023

Thesis Supervisor: Asst. Prof. Nur Mustafaoglu

Keywords: mesenchymal stem cells, neuronal differentiation, multi electrode arrays, graphene nanoplatelets

Study of neurological pathology mechanisms is essential to understand and create therapies of neurological disorders. However, due to the human brain's complexity and inaccessibility, research is limited. Additionally, there isn't a well established neuronal cell line available and animal studies fail to reflect physiology of human brain disorders. To address these limitations, stem cell technologies are being developed to create more accurate disease models. Mesenchymal stem cells have emerged as a preferred option for neuronal differentiation due to their multipotency, accessibility, and low immune response properties. Various methods have been employed to differentiate mesenchymal stem cells into neurons, but it is crucial to ensure that the resulting neurons possess functional characteristics resembling a complete neuronal unit within the model. In this study, we describe the process of differentiating human bone marrow-derived mesenchymal stem cells into neurons using a specific differentiation medium supported with extracellular matrix components. We evaluate the functionality of these differentiated neurons using multielectrode arrays, providing possible valuable insights for future research in this field.

ÖZET

İNSAN KEMİK İLİĞİ KAYNAKLI MEZENKİMAL KÖK HÜCRELERDEN İŞLEVSEL NÖRONLAR

EDA KUŞ

Moleküler Biyoloji, Genetik ve Biyomühendislik YÜKSEK LİSANS TEZİ,
Temmuz 2023

Tez Danışmanı: Dr. Öğr. Üyesi Nur Mustafaoğlu

Anahtar Kelimeler: mezenkimal kök hücre, nöronal farklılaşma, çok elektrotlu diziler, grafen nanoplatelet

Nörolojik patoloji mekanizmalarının incelenmesi, nörolojik bozuklukların anlaşılması ve tedavilerinin oluşturulması için kritiktir. Buna rağmen, insan beyninin karmaşıklığı ve erişilemezliği nedeniyle bu alandaki araştırmalar sınırlıdır. Ayrıca, yeterince donanımlı şekilde üretilmiş nöronal hücre hattı bulunmamakta ve hayvan çalışmaları da insan beyni hastalıklarının fizyolojisini kapsamlı yansıtamamaktadır. Bu sınırlamaları aşmak ve gerçeğe daha yakın hastalık modelleri oluşturmak için kök hücre teknolojileri geliştirilmektedir. Mezenkimal kök hücreler, birden çok hücreye farklılaşabilmeleri, erişilebilirlikleri ve düşük bağışıklık tepkisi yaratmaları özellikleri nedeniyle nöronal farklılaşma yöntemleri için tercih edilen bir seçenek olarak ortaya çıkmıştır. Mezenkimal kök hücreleri nöronlara farklılaştırmak için çeşitli yöntemler kullanılmış olsa da, elde edilen nöronların model içinde sağlıklı ve bütün bir nöronal birim gibi işlevsel özelliklere sahip olduğundan emin olmak önemlidir. Bu çalışmada, insan kemik iliğinden elde edilmiş mezenkimal kök hücrelerinin ekstraselüler matriks bileşenleri ile desteklenen bir süreçle nöronlara farklılaştırılma sürecini tanımlıyoruz. Bu farklılaşmış nöronların işlevselliğini çok elektrotlu diziler kullanarak değerlendiriyor ve bu alandaki gelecekteki araştırmalar için olası değerli içgörüler sunuyoruz.

ACKNOWLEDGEMENTS

I would like to express my gratitude to all those who have been by my side throughout this journey of completing my master's thesis.

Firstly, I am forever thankful for my supervisor, Dr. Nur Mustafaoglu, for her guidance. As an esteemed professional and a woman in STEM, her dedication, achievements, and passion have been a constant inspiration for me. She has always believed in my capabilities even when I did not. She is not only a role model but also a mentor to me, and I will look up to her forever.

I would also like to thank Dr. Nasrollah Tabatabaei for his support and insights during the project, which provided more depth to this thesis.

I also acknowledge the financial support of TUBITAK for the project "Developing an in vitro human epilepsy-on-a-chip model equipped with an intact blood-brain barrier for screening anti-epileptic drugs (121N158)" and MSCA-WF (101028391) that made this thesis possible. The contribution of this support cannot be overstated.

To my dear family, I am deeply thankful for always prioritizing my education and being by my side through all the challenges of life. I cannot thank you enough.

Lastly, I would like to thank all my friends who have believed in me. There were many days when they provided me with motivation and support. I want to especially mention Gülin Baran, who has been both a dear friend and a mentor to me on this journey. I will forever cherish the times we had together, and I am thankful for the journey that led me to gain a new lifelong friend.

In conclusion, I have completed this thesis with the support and efforts of the individuals mentioned above, along with others who have contributed to my master's journey.

Dedication page
I dedicate this thesis to my beloved family.

TABLE OF CONTENTS

LIST OF TABLES	x
LIST OF FIGURES	xi
LIST OF ABBREVIATIONS	xiv
1. INTRODUCTION	1
1.1. Animal Model Limitations	2
1.2. Stem Cell Technology and Neurological Disease Modelling	3
1.2.1. Mesenchymal Stem Cells	4
1.2.1.1. Neuronal Differentiation of Mesenchymal Stem Cells	6
1.3. Use of Extracellular Matrix Components in Differentiation	8
1.3.1. Graphene Oxide and Graphene Nanoplatelets in Neuronal Dif-	
ferentiation	9
1.4. Multielectrode Arrays for Characterization of Differentiated Neurons.	11
2. AIM OF THE STUDY	13
3. MATERIALS AND METHODS	14
3.1. Materials	14
3.1.1. Equipment	14
3.1.2. Reagents	15
3.1.3. Media	16
3.1.4. Solutions and Buffers.....	17
3.2. Methods	18
3.2.1. Freezing and Thawing of bm-hMSCs.....	18
3.2.2. Seeding of bm-hMSCs	18
3.2.3. Coating.....	19
3.2.4. Differentiation.....	19
3.2.5. Immunofluorescent Staining	20
3.2.6. MEA Recording and Analysis.....	21

3.2.7. MTT Cell Viability Assay	23
4. RESULTS	24
4.1. Culturing conditions affect survival and differentiation efficiency.	24
4.2. Gelatin supports cell attachment and proliferation during neuronal differentiation.	26
4.3. GNP and Gelatin Coating Affects Neuronal Marker Expression in bm-hMSCs	28
4.4. Differentiated neurons express Nestin and MAP2	30
4.5. Coating affects neuronal activity response to KCl.	32
4.6. KCl does not generate response from bm-hMSCs	38
5. DISCUSSION	40
BIBLIOGRAPHY	45
APPENDIX A	52

LIST OF TABLES

Table 3.1. Differentiation Medium Contents and Volume	17
---	----

LIST OF FIGURES

Figure 1.1. Differentiation potential of bone-marrow derived mesenchymal stem cells into multiple lineages.....	4
Figure 1.2. Minimum criteria by the ISCT to indentify human MSCs.	5
Figure 1.3. Neuronal Differentiation of MSCs isolated from human bone marrow application in disease modelling and drug screening.	7
Figure 1.4. ECM stiffness effects differentiation of MSCs.....	8
Figure 1.5. Graphene Nanoplatelets are produced from graphite.....	10
Figure 3.1. Differentiation protocol timeline.....	19
Figure 3.2. Medium change angle.....	20
Figure 3.3. MEA Recording Protocol.....	21
Figure 3.4. MEA (a) 60EcoMEA, MultiChannel Systems. (b) Ring attached the MEA and the inlet (shown with arrow).	21
Figure 3.5. Individual electrodes are selected from the MEA (a) MEA layout, (b) corresponding MEA reader compartment layout, (c) placement of the compartment on the reader.	22
Figure 3.6. Individual electrodes are selected from the layout. (a) Electrode numbers of the MEA, (b) corresponding compartment layout on the reader, (c) compartment's placement on the reader	22
Figure 4.1. bm-hMSCs seeded at 3.000 cells/cm ² density show neurological morphology on day 3 of differentiation. Cell detachment and death occurs on day 4 of differentiation.....	24
Figure 4.2. Optimal seeding density accelerates neurological morphology change. Cells seeded at (a) 10.000 cells/cm ² , (b) 6.000 cells/cm ² , (c) and 3.000 cells/cm ² density after 24h of induction using single step cytokine-based neuronal differentiation medium.	25
Figure 4.3. Medium change conditions affect cell death. Cells on day 4 of neuronal induction with conditions (a) complete change every 48h, (b) 1:2 change every 24h, and (c) 1:2 change every 24h.....	25

Figure 4.4. Brightfield images of MSCs on day 5 of induction on different coating materials show 0.1% gelatin coating decrease cell detachment and improve cell proliferation while collagen IV does not. (a) Differentiated cells on day 5 of induction on (a) uncoated, (b) 0.1% Gelatin coated, and (c) 10 μ g/mL collagen coated plate.	26
Figure 4.5. Gelatin concentration affects neuronal marker MAP2 expression. MAP2 immunostaining images processed using CellProfiler CorrectIllumination module for (a) 0.1% gelatin coating, (b) 0.2% gelatin coating, and (c) 0.4% gelatin coating. (d) IntegratedIntensity measurement comparison graph.	27
Figure 4.6. bm-hMSCs express neuronal markers MAP2 and Nestin. Fluorescent images of neuronal protein expression and DAPI staining. ...	28
Figure 4.7. MTT cell viability assay for GNP concentrations.	29
Figure 4.8. MAP2 and Nestin marker expression on bm-hMSCs with gelatin and GNP coating.	29
Figure 4.9. bm-hMSCs on gelatin and GNP coating shows significant increase in expression of neuronal marker Nestin. MAP2 and Nestin expression calculated by Integrated Intensity using Two-way ANOVA analysis, p value= 0,0015 and 0,0006.	30
Figure 4.10. Nestin and DAPI staining for cells on day 4 of differentiation. On (a) no coating, (b) gelatin coating, and (c) GNP coating.	31
Figure 4.11. MAP2 and DAPI staining for cells on day 4 of differentiation. On (a) no coating, (b) gelatin coating, and (c) GNP coating.	31
Figure 4.12. Nestin and MAP2 marker expression analysis using Integrated Intensity per surface are shows no significant difference on differentiated cells among coating conditions . (a) Representative CellProfiler Module for cell selection and analysis. (b) MAP2 and Nestin expression calculated by Integrated Intensity per surface area using Two-way ANOVA analysis.	32
Figure 4.13. 5 minutes of spiking activity on electrode 2 and electrode 6. Neruons at day 4 of differentiation. 15 mM KCl added at 57 th second.	34
Figure 4.14. Temporal distribution of activity in rater plot for electrode 2 and electrode 6 for cells on day 4 of differentiation show synchronization. 5 KHz sampling rate.	34
Figure 4.15. Corresponding electrode locations on the MEA surface.	35
Figure 4.16. Neurons at day 4 of differentiaiton on a 0.2% gelatin coated MEA show increased spiking activity. 5 KHz sampling rate.	35

Figure 4.17. Neurons at day 7 of differentiation on a GNP coating show distinct temporal distribution in spiking activity in response to 15 mM KCl treatment. 86,46 seconds long period that records no spiking activity shown with blue line on the temporal distribution raster plot. 5 KHz sampling rate.	36
Figure 4.18. Neurons spiking activity on electrode 7 at day 7 of differentiation on 2% Gelatin coating to 15 mM KCl treatment added at 52 nd second.	37
Figure 4.19. Neurons spiking activity on electrode 7 and on electrode 6 at day 7 of differentiation on 2% Gelatin coating in response to 30 mM KCl treatment added at 30 th second.	37
Figure 4.20. Neurons on gelatin coating at day 7 of differentiation respond to 30 mM KCl with increased spiking activity. (a) Temporal distribution of spiking activity on in response to 15 mM KCl, (b) in response to 30 mM KCl treatment on electrode 7, and (c) in response to 30 mM KCl treatment on electrode 6. Sampling rate 5 KHz.	38
Figure 4.21. bm-hMSCs do not respond to 15 mM KCl added at the 38 th second.	39

LIST OF ABBREVIATIONS

AD Alzheimer's Disease	2
ALS Amyotrophic Lateral Sclerosis	2
BBB Blood Brain Barrier	1
bm-hMSCs Bone-marrow Derived Human Mesenchymal Stem Cell	4
bmSCs Bone-marrow Derived Mesenchymal Stem Cell	4
BMVECs Brain Microvascular Endothelial Cells	1
CNS Central Nervous System	1
ECM Extracellular Matrix	6
EEG Electroencephalography 1	11
ESC Embryonic Stem Cells	3
GFAP Glial fibrillary acidic protein	10
hNSC Human Neural Progenitor Stem Cell	10
iPSCs Induced Pluripotent Stem Cells	3
ISTC International Society for Cellular Therapy	5
MEA Multi Electrode Array	32
PSC Pluripotent Stem Cells	3
SOD1 Superoxide Dismutase	2

1. INTRODUCTION

In 2016, neurological disorders were identified as the leading cause of disability-adjusted life years and the second leading cause of death. Aging is the number one factor that is driving the numbers of neurological disorders higher, which means the burden will only increase with the ageing population (Feigin, 2019). The increase of neurological disorder burden creates a high demand for new therapies. The lack of successful treatments and understanding of disease mechanisms suggests there is much to discover about neurological diseases. The inaccessibility of the human brain to study led our knowledge so far to be built on postmortem tissue and animal model studies that do not recapitulate the complete mechanisms (Little, Ketteler, Gissen & Devine, 2019). Drug discovery and development is a heavily regulated, highly labor-intensive field, with possible low success rates. The failure rates for central nervous system CNS diseases are very high compared to other areas of drug discovery (Gribkoff & Kaczmarek, 2017). Especially, neurodegenerative diseases where most drugs are reported to have effects on symptoms but not the disease progression itself (Stanzione & Tropepi, 2011), (Berk & Sabbagh, 2013). A study by the Tufts University Center for the Study of Drug Development shows that the marketing approval by the FDA of CNS drugs is less than the half of the non-CNS drugs. The study also points out that the development time of CNS drugs is much greater than other drugs. There are multiple factors that cause the low success rates for CNS drugs. Firstly, the human brain is protected by highly selective and unique blood-brain barrier BBB. The BBB is formed by endothelial cells lining the cerebral capillaries together with astrocytes, perivascular neurons and pericytes. By controlling the transport between the blood and the CNS, the BBB maintains the homeostasis of the brain for an optimal functioning. Brain microvascular endothelial cells BMVECs form complex tight junctions that seals the paracellular pathway, making the transcytosis required to be used to transport molecules from the blood into the CNS (Cecchelli, Berezowski, Lundquist, Culot, Renftel, Dehouck & Fenart, 2007). These tight junctions are created by transmembrane proteins occludin, the claudins and the junctional adhesion molecules. The transmembrane proteins are linked to the actin cytoskeleton by cytoplasmic accessory proteins including zonula

occludin protein 1 (ZO-1), ZO-2 and cingulin and allow modulation of paracellular transport (Huber, Egleton & Davis, 2001). The BBB holds a clinical relevance in both its optimal function and dysfunction. Many neurological disorders show dysfunction in BBB (Wu, Sonninen, Peltonen, Koistinaho & Lehtonen, 2021), while the optimal function limits the crossing of drugs (Mason, 2015). CNS drugs are usually not taken into clinical trials if some mechanism for CNS entry is not demonstrated (Gribkoff & Kaczmarek, 2017).

1.1 Animal Model Limitations

The lack of animal models is another limitation in CNS research. The animal models present low predictive validity even if they are recreating the disease to a certain level (Hurko & Ryan, 2005). This was said to be most frequently reported problem for the CNS drugs to fail in the clinic (Gribkoff & Kaczmarek, 2017). For example, Alzheimer's Disease (AD) animal models express mutations associated with the human disease. Since spontaneous development of AD-like hallmarks is not observed in aging rodents the contribution of these animals to the research requires alterations by either neurochemically or morphologically. Altered amyloid or tau protein processes cause these animals to express AD-like β -amyloid plaques, tau tangles or, both. Although both the β -amyloid plaques, tau tangles are established markers for AD, the clinical development for a candidate drug is still limited by; difference in pharmacology of the drug in the animal model and humans, difference in neurotransmitter wiring in the human brain and the animals, and lastly the difference in the metabolism of said drug (Van Dam & De Deyn, 2011). Another example for animal models not translating into humans can be given for Amyotrophic Lateral Sclerosis (ALS). A large number of studies that used mice with ALS-like symptoms achieved by overexpression of mutated form of the superoxide dismutase (SOD1) gene failed the clinical trials (Gordon & Meininger, 2011).

1.2 Stem Cell Technology and Neurological Disease Modelling

The initial step for disease modelling and drug discovery is the selection of an appropriate cell lines (Little et al., 2019). Neurons especially present a challenge here, due to their inaccessibility and their inability to proliferate in culture. Primary culture needs to be generated from embryonic or early postnatal brains every time (Sahu, Nikkilä, Lågas, Kolehmainen & Castrén, 2019). To overcome this barrier, many models have been based on the use of immortalized or cancer-derived cells. Using these cell lines for neurodegenerative disease modelling have their own limitations as well (Xicoy, Wieringa & Martens, 2017). Immortalized cells are prone to genetic changes and have heterogeneous population (Urraca, Memon, El-Iyachi, Goorha, Valdez, Tran, Scroggs, Miranda-Carboni, Donaldson, Bridges & others, 2015).

Stem cells are unspecialized cells that exist in both embryos and adults with ability to differentiate into other cells of an organism. The specialization of these cells includes several steps. Their ability to differentiate into lineages, their potency, reduces with each step. A unipotent stem cell will differentiate into only one cell type. A spermatogonial stem cell is an example of a unipotent stem cell. Spermatogonial stem cells have the ability to self-renewal but can only differentiate into a single cell type, a sperm. Multipotent stem cells differentiate into mature cell types of their tissue of origin. Hematopoietic stem cells which can develop into all types of blood cells are a type of multipotent stem cell. The highest differentiation potential is held by totipotent stem cells that can differentiate into every cell type of the organism including embryo and extra-embryonic structures. The zygote formed after a sperm fertilizes an egg is a totipotent stem cell. This cell can then develop into three germ layers or form the placenta. 4 days after fertilization, the inner mass of the blastocyst becomes pluripotent. Pluripotent stem cells (PSC) are obtained from this structure. Pluripotent stem cells can form all germ layers but not the embryonic structures. There are two types of pluripotent stem cells. Induced pluripotent stem cells (iPSCs) and Embryonic stem cells (ESC). ESCs are derived from pre-implantation embryos and are a topic of debate due to their source (Zakrzewski, Dobrzyński, Szymonowicz & Rybak, 2019; De Los Angeles, Ferrari, Xi, Fujiwara, Benvenisty, Deng, Hochedlinger, Jaenisch, Lee, Leitch & others, 2015). iPSCs are generated by reprogramming somatic cells by expression of four transcription factors named “Yamanaka factors”: Oct4, Sox2, Klf4 and c-Myc (Yu, Vodyanik, Smuga-Otto, Antosiewicz-Bourget, Frane, Tian, Nie, Jonsdottir, Ruotti, Stewart & others, 2007; Takahashi, Tanabe, Ohnuki, Narita, Ichisaka, Tomoda & Yamanaka, 2007).

1.2.1 Mesenchymal Stem Cells

Mesenchymal stem cells (MSCs) are one of the most promising cell types studied for central nervous system diseases due to their multipotency, accessibility and low immune response properties (Pittenger, Mackay, Beck, Jaiswal, Douglas, Mosca, Moorman, Simonetti, Craig & Marshak, 1999) (Woodbury, Schwarz, Prockop & Black, 2000). Most significantly, MSCs can be obtained from bone marrow (Jones, Kinsey, English, Jones, Straszynski, Meredith, Markham, Jack, Emery & McGonagle, 2002a), adipose tissue (Aust, Devlin, Foster, Halvorsen, Hicok, Du Laney, Sen, Willingmyre & Gimble, 2004), placenta (Adani, Basheer, Hailu, Fogel, Israeli, Volinsky & Gorodetsky, 2019), Wharthon’s jelly of the umbilical cord (Wang, Hung, Peng, Huang, Wei, Guo, Fu, Lai & Chen, 2004), natal teeth (Karaöz, Doğan, Aksoy, Gacar, Akyüz, Ayhan, Genç, Yürüker, Duruksu, Demircan & others, 2010), and more28–30. So far in central nervous system repair studies, bone-marrow derived MSCs (bmSCs) and adipose-derived MSCs are the most extensively studied cell sources (Kaminska, Radoszkiewicz, Rybkowska, Wedzinska & Sarnowska, 2022).

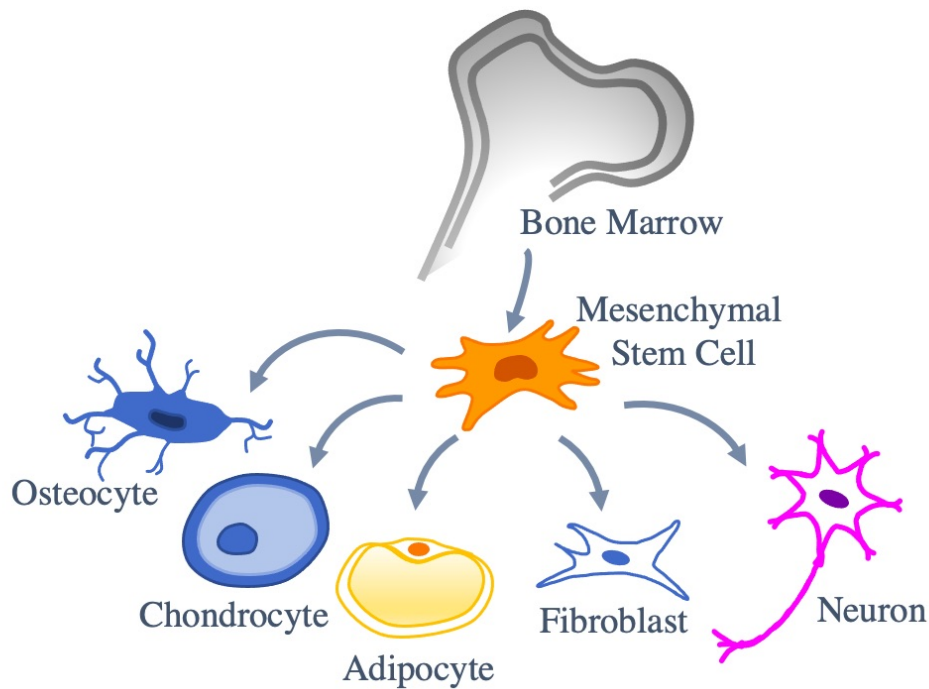


Figure 1.1 Differentiation potential of bone-marrow derived mesenchymal stem cells into multiple lineages.

The two main stem cell populations that are isolated from bone marrow are hematopoietic stem cells and bone-marrow derived human MSCs (bm-hMSCs) (Méndez-Ferrer, Michurina, Ferraro, Mazloom, MacArthur, Lira, Scadden, Ma’ayan, Enikolopov & Frenette, 2010). The ability of bm-hMSCc to adhere physically to the plastic cell culture plate surface is their most important property that is used in their isolation and purification process (Tondreau, Lagneaux, Dejeneffe, Delforge, Massy,

Mortier & Bron, 2004). The isolation and enrichment methods vary from antibody-based cell sorting, low/high density culture techniques, positive and negative selection method, changing the medium frequently and to enzymatic digestion (Li, Zhang & Qi, 2013; Jones, Kinsey, English, Jones, Straszynski, Meredith, Markham, Jack, Emery & McGonagle, 2002b). But, the gold standard method has been described by Pittenger for the isolation (Pittenger et al., 1999). Isolated MSCs need to fulfill certain criteria regardless of their isolation method, as summarized in Figure 1.2. This criteria have been proposed by Mesenchymal and Tissue Stem Cell Committee of the International Society for Cellular Therapy (ISTC). By this criteria, MSCs are defined as plastic-adherent cells when they are maintained in standard culture conditions. They also should express CD105, CD73, CD90, and lack expression of CD45, CD34, CD14, CD11b, CD79 alpha or CD19 and HLA-DR surface molecules. Lastly, they should have the ability to differentiate into osteoblasts and adipocytes in vitro (Dominici, Le Blanc, Mueller, Slaper-Cortenbach, Marini, Krause, Deans, Keating, Prockop & Horwitz, 2006).

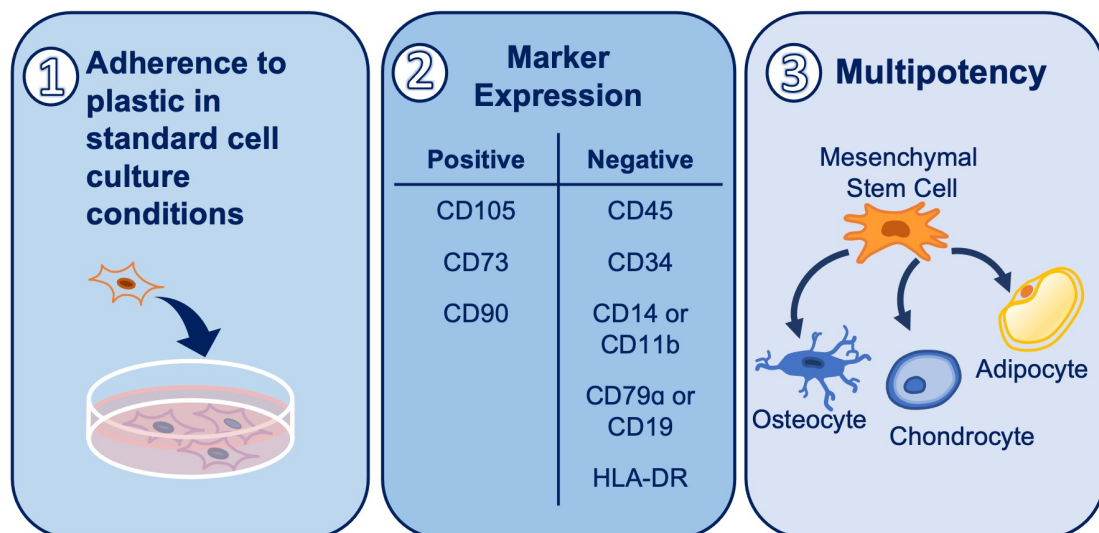


Figure 1.2 Minimum criteria by the ISCT to identify human MSCs.

Adherence to plastic is one of the main criteria because it is a feature that is expressed even by specific subsets of MSCs (Colter, Class, DiGirolamo & Prockop, 2000). Even when MSCs are maintained and expanded without adherence under very specific conditions (Baksh, Davies & Zandstra, 2003), these cells are expected to show plastic adherence under standard cell culture conditions to meet the criteria by the ISTC to be considered as a population of MSCs. Expression of surface Ag is a popular method in immunology and hematology used to identify a cell population rapidly. ISTC guideline proposes that MSCs must express CD105, CD73 and CD90. CD105, also known as endoglin, is a cell membrane glycoprotein that binds several factors of Transforming Growth Factor (TGF)-beta superfamily (Fonsatti, Sigalotti,

Arslan, Altomonte & Maio, 2003). CD73 is a membrane bound enzyme also known as ecto-5'-nucleotidase. CD73 catalyzes the conversion of adenosine monophosphate into adenosine (Zimmermann, 1992). High expression of CD73 was associated with MSCs anti-inflammatory activity (Tan, Zhu, Zhang, Ouyang, Tang, Zhang, Qiu, Liu, Ding & Deng, 2019). CD90, also known as Thy-1, is a membrane anchored protein that was first identified on mouse T lymphocytes (Pont, 1987). In order to obtain a MSC population that does not contain other type of cells, they are negatively selected by expression of Ag specific to cell types commonly found in a MSC culture. CD45 is a membrane glycoprotein found in leukocytes (Nakano, Harada, Morikawa & Kato, 1990). CD34 marks predominantly hematopoietic stem cells, hematopoietic progenitor cells and endothelial cells (Sidney, Branch, Dunphy, Dua & Hopkinson, 2014). CD14 and CD11b mark mature circulating monocytes and macrophages(Lambert, Preijers, Yanikkaya Demirel & Sack, 2017). CD79 and CD19 are markers for B cells, they act as a key component of the B cell antigen receptor complex and dominant signaling component respectively ((Van Noesel, Van Lier, Cordell, Tse, Van Schijndel, De Vries, Mason & Borst, 1991); (Wang, Wei & Liu, 2012).

1.2.1.1 Neuronal Differentiation of Mesenchymal Stem Cells

Multiple methods have been reported to be employed for differentiation of MSCs into neurons. These strategies can be divided mainly into four categories such as use of psychotropic drugs, small molecules, enriched media, and epigenetic modifications. Alternative methods contain using extracellular matrix (ECM) components and co-culture conditions as a strategy to mimic the brain environment (Lee, Seo, Lee, Jang, Kim & Sung, 2018; Hernández, Jiménez-Luna, Perales-Adán, Perazzoli, Melguizo & Prados, 2020).

The use of growth factors, also sometimes referred as cytokines, and/or chemicals is the primarily employed method for differentiation of MSCs. Until 2000, differentiation potential of bm-MSCs into osteocytes, myocytes, chondrocytes, and adipocytes in vitro were discovered (Prockop, 1997; Kuznetsov, Friedenstein & Gheron Robey, 1997; Ferrari, Cusella, Angelis, Coletta, Paolucci, Stornaiuolo, Cossu & Mavilio, 1998). Then in 2000, it was reported that rodent and human MSCs can differentiate into neurons (Woodbury et al., 2000). This paper used 2-Mercaptoethanol (β ME) to induce the neuronal differentiation. β ME induced cells expressed Nestin as an early neuronal marker, then trkA which is a neuron growth factor receptor. The

differentiated cells also had morphological traits such as long neurite-like extensions.

Some psychotropic drugs such as antidepressants were established to improve proliferation and differentiation of neural precursor cells (NPCs)(Nakagawa, 2010). Then in rat bone-marrow MSCs, the use of antidepressants imipramine, desipramine and fluoxetine along with astrocyte-conditioned medium and growth factors EGF and bFGF were shown to improve differentiation efficiency after transplantation (Borkowska, Kowalska, Fila-Danilow, Bielecka, Paul-Samojedny, Kowalczyk & Kowalski, 2015). Citalopram is another antidepressant that is shown to improve bone-marrow derived MSCs neuronal differentiation and increase their proliferation (Verdi, Mortazavi-Tabatabaei, Sharif, Verdi & Shoaee-Hassani, 2014).

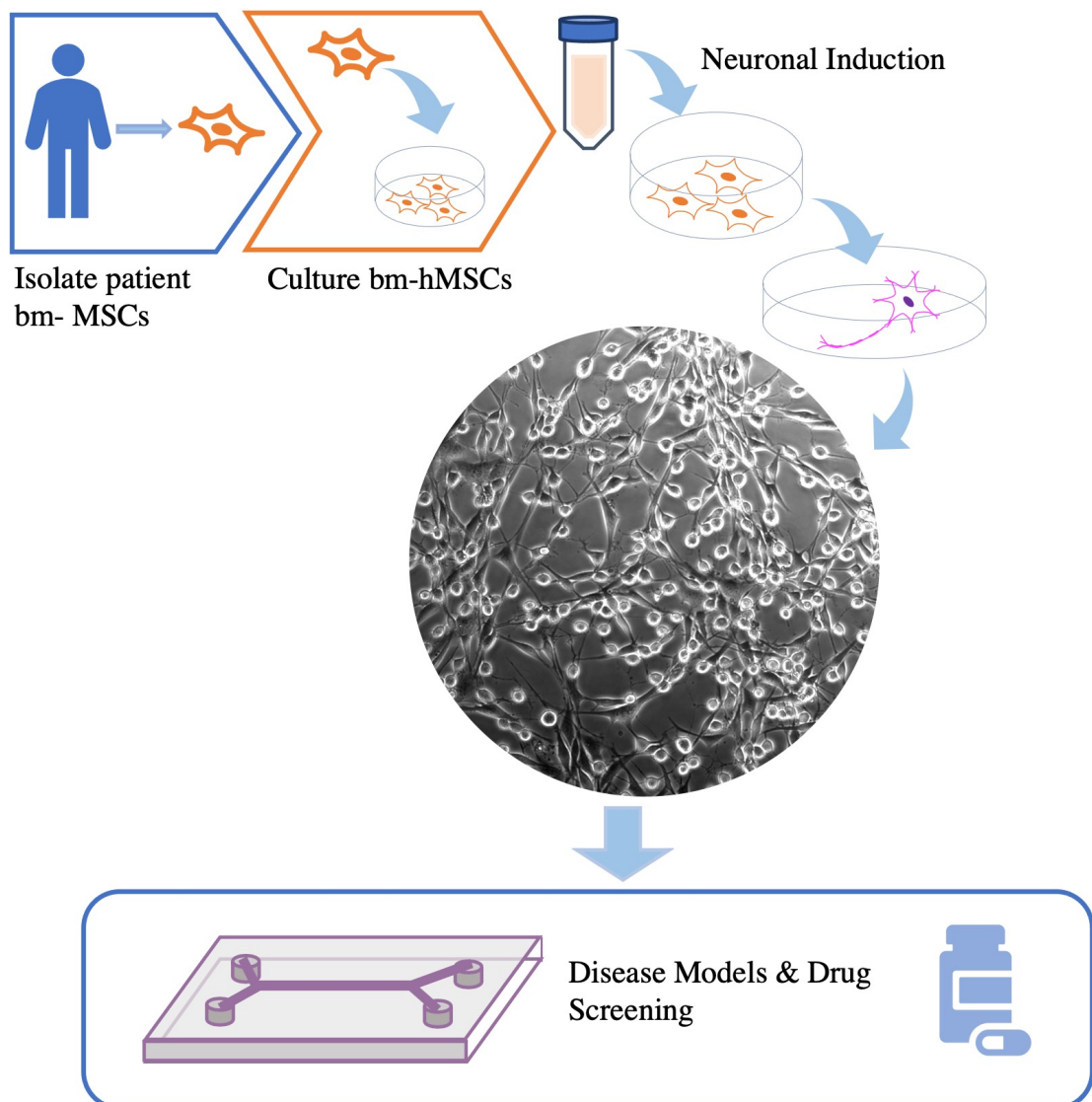


Figure 1.3 Neuronal Differentiation of MSCs isolated from human bone marrow application in disease modelling and drug screening.

1.3 Use of Extracellular Matrix Components in Differentiation

Whilst stem cells' lineage specification by soluble stimuli has been well described (Sobacchi, Palagano, Villa & Menale, 2017), effects of extracellular environment and mechanical forces have also been studied extensively (Patwari & Lee, 2008). MSCs respond to matrix stiffness by initiating mechanotransduction cascades and affecting their differentiation as a result. It has been showed that MSCs will differentiate into different lineages depending on the stiffness of the matrices it is cultured on. Mimicking the stiffness of a brain by soft matrices induce neuronal differentiation and mimicking the stiffness of a muscle by harder matrices induce a myogenic differentiation, and at last, the hardest substrate leads to osteoblast formation by MSCs (1.4) (Engler, Sen, Sweeney & Discher, 2006). Basement membranes fibronectin, laminin, collagen and gelatin provide the extracellular matrix. Fibronectin is shown to improve migration and proliferation while collagen and laminin stimulate attachment and differentiation (Olsen, 2014). Gelatin, a polymer derived from partial hydrolysis of collagen, is known to contain integrin binding sites allowing cell adhesion, migration, and differentiation (Hajiali, Shahgasempour, Naimi-Jamal & Peirovi, 2011).

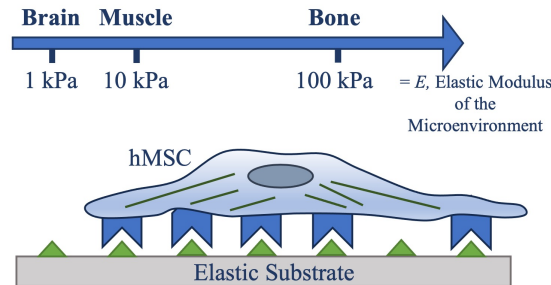


Figure 1.4 ECM stiffness effects differentiation of MSCs.

For neuronal differentiation of stem cells, several papers have investigated the role of ECM. ECM hydrogels derived from the CNS have been demonstrated to support neuronal differentiation of MSCs due to their mechanical properties. The study by Medberry, Crapo, Siu, Carruthers, Wolf, Nagarkar, Agrawal, Jones, Kelly, Johnson & others (2013) that uses the neural cell line N1E-115 sourced from mouse neuroblastoma seeded on ECM hydrogels. They reported that ECM hydrogels obtained from brain, spinal cord, and urinary bladder tissue samples increased all neurites. The biggest neurite length was observed on cells on brain ECM, which was explained as a possible tissue-specific effect. These results suggest the application of ECM in neuronal differentiation of stem cells. The topography of the ECM also participate

in the neuronal differentiation of hMSCs. Yim, Pang & Leong (2007) demonstrated that hMSCs show increase in neuronal marker expression when they are seeded on a surface with nano-gratings. This supports the possible alternative use of ECM, which is through its topography.

1.3.1 Graphene Oxide and Graphene Nanoplatelets in Neuronal Differentiation

In the pursuit of neuronal differentiation of stem cells, graphene and graphene oxide (GO) products have been studied due to their unique characteristics. Graphene is a two-dimensional carbon-based nanomaterial with carbons packed as a single layer in hexagonal shape. Graphene and its derivatives GO and reduced GO (rGO) provide outstanding properties such as electrical and thermal conductivity, mechanical strength and large surface area (Shin, Li, Jang, Khoshakhlagh, Akbari, Nasajpour, Zhang, Tamayol & Khademhosseini, 2016). These materials have been used with stem cells to induce their self-renewal and differentiation. GO, the highly oxidized form of graphene, is preferred more over graphene due to its multiple functional groups that provide a way to combine it with other materials. GO has also been reported to be less toxic compared to graphene. GO's effect on bm-hMSC proliferation was studied by Wei, Liu, Jiang, Zeng, Huang & Yu (2017). They reported that 0.1 $\mu\text{g}/\text{mL}$ of GO promotes proliferation of bm-hMSCs significantly. But, concentrations from 1 to 10 $\mu\text{g}/\text{mL}$ reduced cell proliferation and cell size reduced in these higher concentrations.

GO's effect on differentiation of MSCs have been reported by multiple studies. Collectively, GO has been linked to differentiation of MSCs into osteoblasts, adipocytes, chondroblasts, and neurons. Osteogenic differentiation of bm-hMSCs were reported by using cultured in a medium containing ultrasonically dispersed GO nanosheets at 0.1 $\mu\text{g}/\text{mL}$ concentration. GO nanosheet containing medium's osteogenesis effect was explained by activation of Wnt/ β -catenin signaling pathway (Wei et al., 2017). MSCs can also be differentiated into adipogenic cells using GO but the differentiation protocol includes chemical inducers unlike osteogenic differentiation (Patel, Moon, Ko & Jeong, 2016). MSCs multilineage potential allows them to differentiate into neurons. Graphene and graphene products contribute to neuronal differentiation of MSCs due to their electroconductive nature. Among the graphene and its products, rGO is highly the favored one because its oxygen group is reduced and therefore it does not create any disruption in electrical activity. MSCs multilineage potential

allows them to differentiate into neurons. Graphene and graphene products contribute to neuronal differentiation of MSCs due to their electroconductive nature. Among the graphene and its products, rGO is highly the favored one because of its oxygen group is reduced and therefore it does not create any disruption in electrical activity. A study by Lim, Seonwoo, Choi, Jin, Jang, Kim, Kim, Kim, Choung & Chung (2016) applied pulsed electromagnetic field on rGO surface to observe neuronal differentiation of human alveolar bone marrow stem cells and observed increase in neuronal markers Nestin and MAP2. In a study by Yim et al. (2007) neuronal differentiation of hMSCs were achieved using three-dimensional graphene scaffolds in absence of other exogenous factors. Yim et al. (2007) showed that hMSCs cultured in 3-dimensional graphene scaffolds exhibit increase in neuronal markers GFAP, TujI, Nestin, and MAP2 expression and neuronal morphology changes. The high graphene content 3D scaffold creates an environment that allows cells to connect through their neurite extensions and form networks. Another study uses graphene on a glass surface. After human neural progenitor stem cells (hNSC) were seeded on the graphene, the graphene coated glass was transferred into a laminin solution. Then, differentiation was induced by culture medium containing bFGF (10 ng/mL) and EGF (10 ng/mL). hNSCs on graphene substrate exhibited enhanced differentiation, having higher percentage of neurons and a lower percentage of glial cells compared to the hNSCs on the glass surface. Additionally, graphene increased cell adherence (Park, Park, Sim, Sung, Kim, Hong & Hong, 2011).

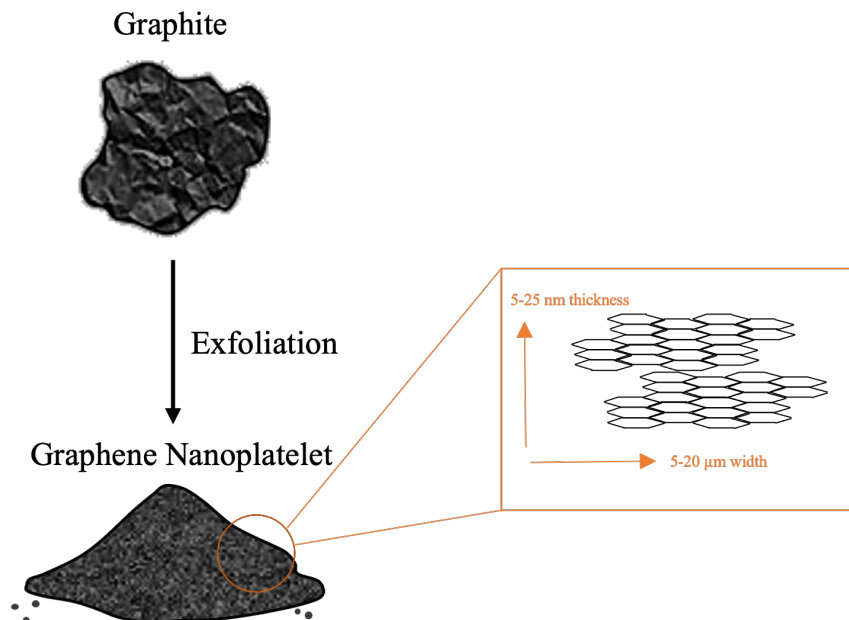


Figure 1.5 Graphene Nanoplatelets are produced from graphite.

Graphene nanoplatelets are another graphene product that contains stacked graphene layers. They are similar to graphene in having mechanical strength, electri-

cal conductivity and thermal conductivity. Graphene nanoplatelets can be produced by multiple methods such as exfoliation of graphite and chemical vapor deposition. In exfoliation method, graphene layers are separated from graphite that creates thin nanoplatelets in result (Novoselov, Geim, Morozov, Jiang, Zhang, Dubonos, Grigorieva & Firsov, 2004). Graphene nanoplatelets are commonly used to incorporate into other materials to enhance their properties (Peng & Zhang, 2021). However, their effect on neuronal differentiation have not been studied extensively.

1.4 Multielectrode Arrays for Characterization of Differentiated

Neurons

When modelling an organ, it is important to capture its properties as close to its nature. Ensuring accuracy in models requires well established and robust differentiation protocols. For neurons derived from stem cells, the characterization and the assessment can't rely solely on neuronal marker expression. Neurons are special cells that generate action potentials, form synaptic connections, and show networking activity through those formed connections (Chanda, Ang, Davila, Pak, Mall, Lee, Ahlenius, Jung, Südhof & Wernig, 2014). This firing behavior has been studied extensively both in vitro and in vivo by methods such as use of multi electrode arrays (MEA), electroencephalography (EEG) (Buzsáki, Anastassiou & Koch, 2012), patch-clamp (Stuart, Dodt & Sakmann, 1993) and various calcium dependent dyes (Grienberger & Konnerth, 2012).

MEAs are made up of electrodes arranged on a surface that can record electrical activity of a cell culture or a tissue. MEAs have been used for recordings on the human brain commonly, therefore there is a substantial knowledge to refer to for use in stem cell studies (Marg & Adams, 1967). Some studies have also been compared to EEG recordings but can be more complicated than MEA data comparison (Trujillo, Gao, Negraes, Gu, Buchanan, Preissl, Wang, Wu, Haddad, Chaim & others, 2019). MEA recordings provide significant advantages such as being noninvasive and much less complicated compared to methods like clamp recordings. This also means they can be applied easily in more complicated devices like microfluidic chips. An MEA recording also does not require dyes like calcium indicators therefore the cell viability can be preserved throughout the protocol (Kamioka, Maeda, Jimbo, Robinson & Kawana, 1996). Lastly, MEAs provide recordings taken at the same time on electrodes different locations which gives insight on network activity of the

differentiated neurons in a culture (Kizner, Fischer & Naujock, 2019).

Electrode diameters on an MEA surface can vary from a few to tens of micrometers (Ahmadvand, Mirsadeghi, Shanehsazzadeh, Kiani & Fardmanesh, 2020). This range in diameter allows customization for different parts of the neuron like its soma or neurite. Electrical signals created by neuronal firings are usually referred as “spikes” or “spiking activity” which are recorded by the electrodes (Buzsáki et al., 2012). These spikes are then processed by application of a band pass filter. The filter can change depending on the experiment. Common range reported is 300-3000 Hz for spiking activity. A smaller, lower range (1-200 Hz) can be applied to analyze synaptic current behavior which is the flow of ions across one synapse of a neuron to another’s (Harris, Quiroga, Freeman & Smith, 2016).

The most commonly used MEA type is 8X8 on a titanium nitride surface (Multi Channel Systems, MCS GmbH). The base and the electrodes are offered in different materials based on the application purpose. MEAs also have different types that allow uses for specific experiments. There are also multi-well MEAs that allow high-throughput screenings. Additionally, there have been MEA designs that can detect and measure neurotransmitters (Piccolo, Battiato, Bernardi, Plaitano, Franchino, Gosso, Pasquarelli, Carbone, Olivero & Carabelli, 2016).

MEA use for stem cell derived neurons is more wide-ranging for hPSCs instead of MSCs. They have been used to study both basic physiology and pathology of neurons differentiated from hiPSCs. Neurons derived from hiPSCs were used with MEAs to study epileptic behavior, neurotoxicology, hypoxia conditions and genetic disorders (Pelkonen, Pistono, Klecki, Gómez-Budia, Dougalis, Konttinen, Stanová, Fagerlund, Leinonen, Korhonen & others, 2021). In summary, MEAs are useful and promising tools that provide information on neuron populations to support neurological disease modelling studies.

2. AIM OF THE STUDY

This thesis aims to develop a differentiation protocol to obtain functioning neurons from human bone-marrow derived mesenchymal stem cells using chemical inducers coupled with extracellular matrix components such as gelatin and graphene nanoplatelets. For central nervous system studies, current practice is use of induced pluripotent stem cells. But, mesenchymal stem cells are much more accessible and can be less complicated to differentiate which makes them promising candidates in these applications. These stem cell derived neurons are aimed firstly to be in optimum culturing conditions. These optimum culturing conditions are decided by cell attachment and survival rate. Then, the characterization of these obtained neurons are done. First characterization is confirming for neuronal morphology which is defined by neurite extensions, polarized bodies and phase-bright soma. Secondly, neuronal marker expression is confirmed by immunofluorescence staining. Early neuronal marker Nestin and mature neuronal marker MAP2 expressions are measured. Then, in order to assess the representation of a characteristic neuronal behavior, the differentiated neurons are cultured on multi electrode arrays to record spiking activity induced with membrane depolarization via KCl.

3. MATERIALS AND METHODS

3.1 Materials

3.1.1 Equipment

- Autoclave (HiClave HV110, Hirayama, Japan)
- Biological Safety Cabinet (HeraSafe HS15, Heraeus, Germany)
- Centrifuge (5418R, Eppendorf, Germany)
- Centrifuge (5702, Eppendorf, Germany)
- Centrifuge (5415R Eppendorf, Germany)
- CO2 Incubator (Binder, Germany)
- Electronic Balance (AS 220.R2, RADWAG Wagi Elektronicze, Poland)
- Heat block (HP88857105, Thermo Scientific, USA)
- Hemocytometer (Neubauer Improved, Isolab, Germany)
- Vortex Mixer (VM-370, INTLLAB, Türkiye)
- Microscope (Axio Vert.A1, Carl Zeiss, Germany)
- Microscope (Primovert, Zeiss, Germany)
- -80 Freezer (Forma 88000 Series, Thermo Fischer Scientific, USA)

- Safety Cabinet

3.1.2 Reagents

- 3-Isobutyl-1-methylxanthine (Sigma-Aldrich, #I5879)
- B27 supplement (Thermo Fisher Scientific, #17504044)
- Collagen IV (PAN, #LS0004186)
- CoraLite488-conjugated Goat Anti-Rabbit IgG(H+L) 1:1000 (ProteinTech, #SA00013-2)
- Cy3-conjugated Affinipure Goat Anti-Rabbit IgG(H+L) (ProteinTech, #SA00009-1)
- DAPI (ready-made solution) 1:1000 (Sigma-Aldrich, #MBD0015)
- Dibutyryl cyclicAMP (Sigma, #D0627)
- DMEM Low glucose (Gibco, #11054020)
- DPBS with calcium and magnesium (Pan-biotech, #P04-35500)
- DPBS without calcium and magnesium (Pan-biotech, #P04-36500)
- Fetal Bovine Serum (Pan-biotech, # P30-3306)
- Fibroblast growth factor-8 FGF-8 (Pepro Tech, #100-25)
- Gelatin from bovine skin (Sigma Aldrich, #G9391)
- hEGF (Sigma-Aldrich, #E9644)
- L-glutamine (200 mM) (Gibco, #25030149)
- MAP2 polyclonal antibody 1:500 (ProteinTech, #17490-1-AP)
- MTT 3-(4,5-Dimethyl-2-thiazolyl)-2,5-diphenyl-2H-tetrazolium Bromide, (Sigma Aldrich, #475989)
- Nerve Growth Factor (R&D systems, #256-GF-100)
- Nestin polyclonal antibody 1:100 (ProteinTech, #19483-1-AP)
- Neurobasal Medium (Gibco, #21103049)

- Paraformaldehyde (Merck, #158127)
- PBS Tablets (BioShop, #PBS404.100)
- Penicillin-Streptomycin (10,000 U/mL) (Gibco, #11548876)
- Recombinant human basic fibroblast growth factor (R&D systems, #233-FB-010)
- Recombinant human brain-derived neurotrophic factor (BDNF) (R&D systems, #248-BDB)
- Trypsin 0.25% /EDTA 0.02%, in PBS w/o: Ca and Mg, w: Phenol red (Pan-biotech, #P10-019100)
- TUBB3-specific Monoclonal antibody 1:200 (ProteinTech, #66375-1-Ig)

3.1.3 Media

MSC Expansion Medium: Expansion medium is prepared with low-glucose DMEM with 10% FBS (heat-inactivated), 2 mM L-glutamine and 1% Pen/Strep. FBS is heat-inactivated by putting the thawed FBS bottle into the water bath set to 56°C for 30 minutes. Then cooled to room temperature, to be aliquoted or frozen.

Differentiation Medium: After reconstituting the reagents, the medium was prepared for 50 mL of volume as shown in Table 3.1. Filtered with a syringe and a 0.22 µm syringe filter. Differentiation medium was always prepared fresh instead of storing in larger volumes.

3-Isobutyl-1-methylxanthine (100 mg stock): The content of the vial is reconstituted with 1000µL DMSO to a concentration of 100 mg/mL. Aliquoted as 15µL per tube and stored at -80°C.

Dibutyryl cyclicAMP (25 mg stock): The content of the vial is reconstituted using 250 µL double-distilled and autoclaved water to a concentration of 100 mg/mL. Aliquoted and stored at -80°C.

Fibroblast growth factor-8 FGF-8 (5µg stock): The content of the vial reconstituted using 50µL double-distilled and autoclaved water to a concentration of 0.1 mg/mL. Aliquoted and stored at -80°C.

hEGF (0.2 mg stock): The content of the vial is reconstituted using 200µL acetic acid to a concentration of 1mg/mL. Aliquoted and stored at -80°C.

Nerve Growth Factor (100 µg stock): The content of the vial is reconstituted using 1000µL DPBS -/- to a concentration of 100 µg/mL. Aliquoted and stored at -80°C.

Recombinant human brain-derived neurotrophic factor BDNF (10µg stock): The content of the vial reconstituted using 40µL double-distilled and autoclaved water to a concentration of 250 µg/mL. Aliquoted and stored at -80°C.

Recombinant human basic fibroblast growth factor (10 µg stock): The content of the vial is reconstituted using 40µL DPBS -/- to a concentration of 250 µg/mL. Aliquoted and stored at -80°C.

Table 3.1 Differentiation Medium Contents and Volume

	Reconstitution Concentration	Desired Concentration	Final Volume
L-glutamine	200 mM	2 mM	500 µL
Dibutyryl cyclicAMP	100 mg/mL	0.125 mM	31 µL
3-Isobutyl-1-methylxanthine	100 mg/mL	0.5 mM	55,5 µL
hEGF	1 mg/mL	20 ng/mL	1 µL
Fibroblast growth factor-8	0.1 mg/mL	10 ng/mL	5 µL
Recombinant human brain-derived neurotrophic factor	250 µg/mL	10 ng/mL	2 µL
Nerve Growth Factor	100 µg/mL	40 ng/mL	20 µL
Recombinant human basic fibroblast growth factor	250 µg/mL	40 ng/mL	8 µL
B27 Supplement		2%	1000 µL
Neurobasal Medium			48377.5 µL

3.1.4 Solutions and Buffers

Blocking and Permeabilization Buffer: For permeabilization, 1.5% Bovine Serum Albumin, 0.01% Tween80 is prepared in DPBS ++. BSA is mixed thoroughly before Tween80 is added. For blocking, 1.5% Bovine Serum Albumin in DPBS ++ is used.

0.2% Gelatin Mixture: In an autoclavable bottle, 1X PBS is prepared with double-

distilled and autoclaved water according to the instructions of the tablets. Then, the gelatin is weighed for needed amount (0.2%) and added to the PBS. Mixed thoroughly, then autoclaved. Let it come to room temperature before storing at 4°C.

GNP coating: In 0.2% Gelatin mixture, 0.2 µg/mL GNP is mixed thoroughly.

Collagen IV coating: Collagen is diluted to 10 µg/ml concentration in 0.01 M HCl.

Solubilization Solution: In a solvent resistant container, 40% (v/v) dimethylformamide (DMF) in 2% (v/v) glacial acetic acid is prepared working in a fume-hood. Then, 16% (w/v) sodium dodecyl sulfate added and dissolved. pH is adjusted to pH 4.7. Stored at room temperature.

3.2 Methods

3.2.1 Freezing and Thawing of bm-hMSCs

The cells were frozen at 1×10^6 /mL using a freezing medium prepared with expansion medium containing 10% DMSO then stored in either liquid nitrogen tank or -80°C. The frozen cells are thawed in water bath set to 37°C avoiding submerging the cap of the cryovial into the water. After 30 to 60 seconds, the contents of the vial are transferred into a 90 mm cell culture dish containing expansion medium.

3.2.2 Seeding of bm-hMSCs

Wells of the plates are covered with appropriate amount of 0.2% gelatin (200 µL for 48-well) and placed into the incubator at 37°C to incubate for 30 minutes. Plates of previously started culture at an 80% confluency are removed from the incubator and the media is aspirated. Then, washed with DPBS- and appropriate amount of 0.25% Trypsin/EDTA solution is added to detach the cells. After 2 minutes of trypsinization inside the incubator, the cell detachment is observed under the

microscope. Gently tapped on the side using the palm of the hand to aid this detachment. Suitable amount of expansion medium is added to inhibit the trypsin. The cell suspension is transferred into a 15 mL conical tube. Using a hemocytometer, the cell number is counted and calculated. Depending on the conditions, needed concentration of suspensions are prepared. Usually, 3000 cells/cm² for MSC controls and 10.000 cells/cm² for differentiation protocol. The plate prepared with gelatin is removed from the incubator after 30 minutes and the gelatin is aspirated without touching the bottom of the well. Then, cells are seeded according to experimental setup. The plates are returned to the incubator at 37°C, 5% CO₂.

3.2.3 Coating

Gelatin and GNP Containing Gelatin Coating: 150 µL of gelatin (for 48 well plate) is placed on the plate and then into the incubator at 37°C for 30 minutes. Then, the remaining gelatin is aspirated. Cells are then seeded according to the protocol. Collagen IV Coating: 150 µL of collagen prepared in HCl is placed on the wells, then incubated for 1 hour in room temperature. After incubation, collagen is removed from the well and the well is washed with DPBS–.

3.2.4 Differentiation

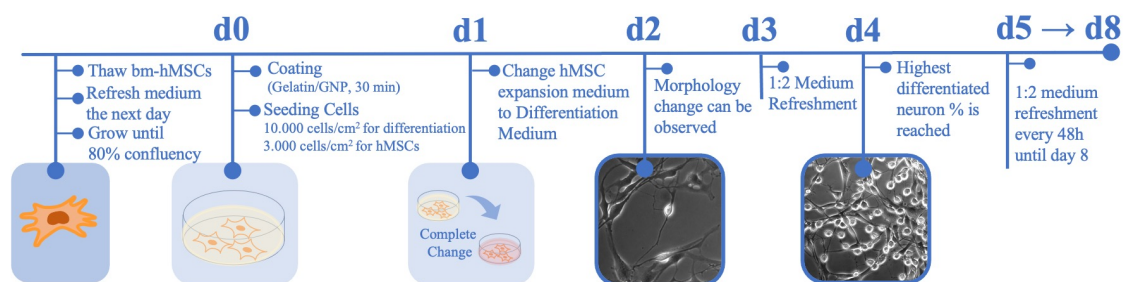


Figure 3.1 Differentiation protocol timeline.

Depending on the conditions of the experiment, cells are seeded onto either 48-well plate or MEA as 10.000 cells/cm² 24 hours after cell seeding, first medium change is done. Neuronal differentiation medium is warmed to 37°C in the water bath. Then, expansion medium is removed from the wells. The neuronal differentiation

medium is added. Cells are returned to the incubator at 37°C, 5% CO₂. 48 hours later, half of the differentiation medium is removed without touching the bottom and aiming at the corner as shown in Figure 3.2 to prevent cell detachment. Fresh differentiation medium is added slowly and by touching the walls of the well. This half change is continued until the end of protocol depending on the experiment.

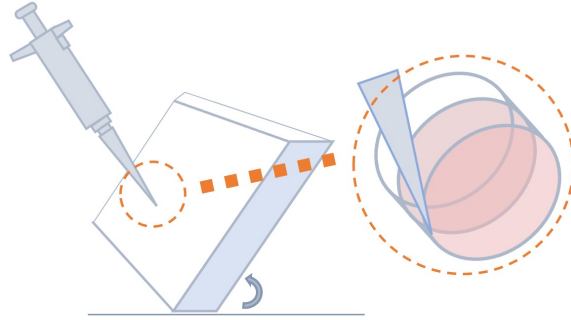


Figure 3.2 Medium change angle.

3.2.5 Immunofluorescent Staining

For the immunofluorescent staining of the cells, the plates were placed on a heating block set to 35°C inside a fume hood. 4% PFA and buffers are pre-warmed to 37°C. All of steps are done in angle shown in Figure 3.2 to prevent cell detachment. Half of the neuronal differentiation medium is removed from the wells and 4%PFA is added at a same volume into the wells slowly by touching the side of the well wall. Then, incubated in dark for 20 minutes still placed on heating block. After incubation, the wells are washed with DPBS++ three times using rocker at the lowest level for 2 minutes. Then, blocking and permeabilization is done using the buffer containing Tween80. The buffer is added and the plate is incubated in dark at room temperature for 2 hours. After incubation, the wells are washed with DPBS++ three times. Then primary antibodies that were prepared according to the dilutions given in 3.1.1 in DPBS++ containing 1.5% BSA are added to the wells and incubated in dark at room temperature for 2 hours. Then, primary antibodies are removed and the wells are washed 3 times with DPBS++. Secondary antibodies prepared in DPBS++ containing 1.5% BSA based on dilutions given in 3.1.1 are added to the wells to be incubated for 1 hour in dark at room temperature. Then the wells are washed with DPBS++ 3 times. DAPI staining is done using DAPI prepared in DPBS++ (1:1000 dilution) and incubating for 2 minutes in dark at room temperature. Then, the wells are washed 3 times with DPBS++. Washing steps are done slowly to avoid cell detachment.

3.2.6 MEA Recording and Analysis

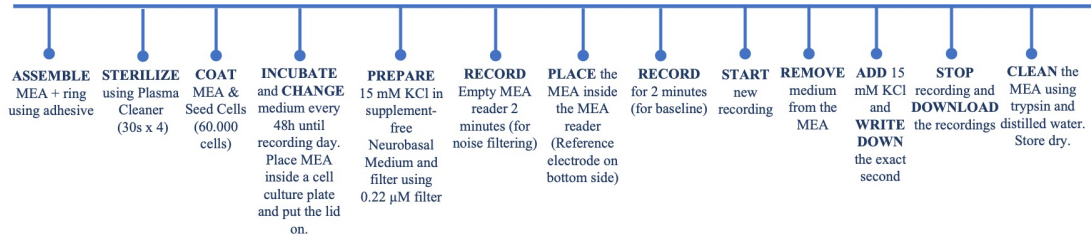


Figure 3.3 MEA Recording Protocol.

MEA is purchased from MultiChannel Systems(#60EcoMEA). The MEA has Gold electrodes and tracks, with internal reference electrode, electrode grid 8x8, 60 electrodes, electrode spacing 700 μ m, electrode diameter 100 μ m (Figure 3.4, a). The purchased MEA does not have a ring. The ring is attached to the MEA surface using clear adhesive. The ring's surface area is 6 cm² and is made of PMMA. The ring contains inlets for medium change using a 200 μ L micropipette tip (Figure 3.4, b).

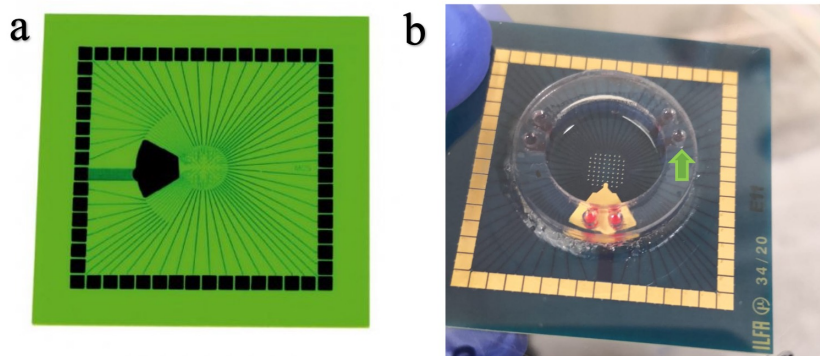


Figure 3.4 MEA (a) 60EcoMEA, MultiChannel Systems. (b) Ring attached the MEA and the inlet (shown with arrow).

The fabrication of the reader compartment (Figure 3.6) has been outsourced by Kavoshgaran Electronic Zenderood, Isfahan, Iran. The reader contains an amplifier, an analog to digital converter and a data processing unit.

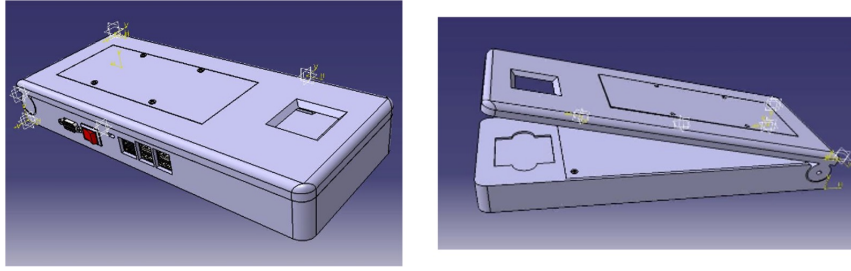


Figure 3.5 Individual electrodes are selected from the MEA (a) MEA layout, (b) corresponding MEA reader compartment layout, (c) placement of the compartment on the reader.

Electrodes are selected from the layout of the MEA (Figure 3.6 a) and the MEA reader's board is prepared accordingly. For example, 7th electrode on the MEA reader (Figure 3.6 b) equals to electrode 75 on the MEA.

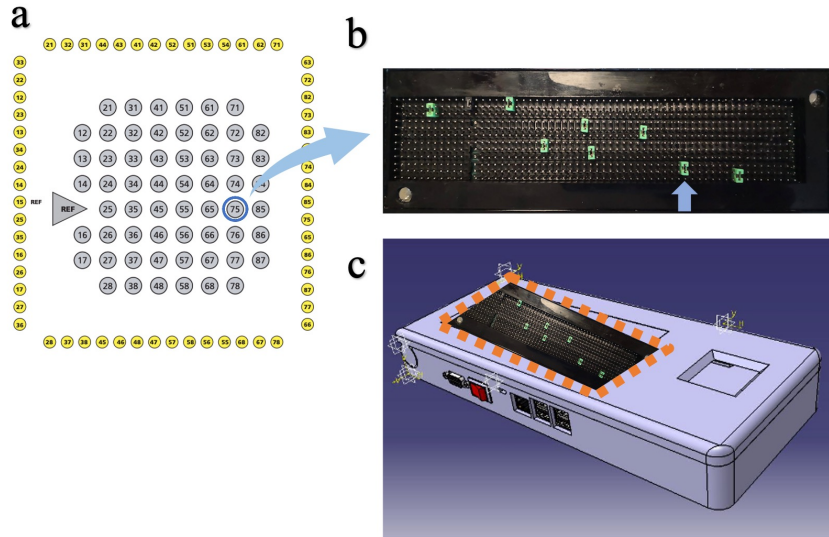


Figure 3.6 Individual electrodes are selected from the layout. (a) Electrode numbers of the MEA, (b) corresponding compartment layout on the reader, (c) compartment's placement on the reader .

MEA is sterilized using a plasma cleaner for 4 times, 30 seconds each. The coating protocol is followed same as coating cell culture plates. Before each experiment, the MEA reader device is ran to record the device background and then the MEA is placed on the device to record a 2 minute baseline. Then, the KCl is given by medium refreshment to record the activity of the neurons. The recorded data is then filtered and used to generate figures using the Matlab code given in appendix. Raster plot is generated using Matlab raster plot function.

3.2.7 MTT Cell Viability Assay

bm-hMSCs are seeded to 96-well plate as previously explained in method 3.2.1 at 10.000 cells per 50 uL of serum-free low-glucose DMEM containing GNP at 0.1 µg/mL, 0.2 µg/mL, 0.4 µg/mL, 2 µg/mL, 5 µg/mL, 10 µg/mL (and 0 µg/mL for control group) concentrations. Conditions are provided in triplicates. Cells are then incubated for 24h in the incubator at 37°C, 5% CO₂. After incubation, cells are treated with 20 µL MTT and incubated at 37°C, 5% CO₂ for 2 hours. After the incubation, 100 µL of solubilization solution is added to the wells. Plate is read at 570 nm.

4. RESULTS

4.1 Culturing conditions affect survival and differentiation efficiency.

To obtain neurons from bm-hMSCs, a cytokine-based differentiation medium (Table 3.1) (Karakaş, Bay, Türkel, Öztunç, Öncül, Bilgen, Shah, Şahin & Öztürk, 2020) was used. Karakaş et al. (2020) reported that the neurons obtained from bm-hMSCs seeded at 3.000 cells/cm² using cytokine-based neuronal differentiation medium were cultured up to day 21. However, when seeded at 3.000 cells/cm² density, and medium change condition was complete refreshment every 48 hours, cell detachment and death was observed on day 4 (Figure 4.1).

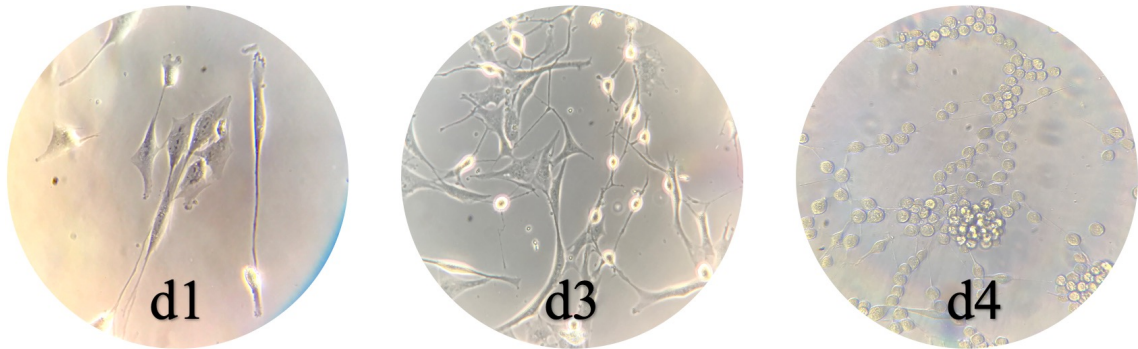


Figure 4.1 bm-hMSCs seeded at 3.000 cells/cm² density show neurological morphology on day 3 of differentiation. Cell detachment and death occurs on day 4 of differentiation.

In order to improve the attachment and cell survival, we optimized the culturing conditions. Neurons seeded at suboptimal density were reported by Anilkumar, Weisova, Schmid, Bernas, Huber, Düssmann, Connolly & Prehn (2017) to go under necrosis while optimal seeding density induced apoptosis in response to glutamate-induced excitotoxicity . To select the optimum seeding density, an experiment was

set up with 3.000 cells/cm², 6.000 cells/cm², and 10.000 cells/cm² cell densities.

Additionally, it has been demonstrated by Wilkins, Kemp, Ginty, Hares, Mallam & Scolding (2009) that human bone marrow-derived MSCs secrete neurotrophic factors that promote neuron survival in vitro through the PI3/Akt pathway. To test the affects of preserved neutrophic factors through less frequent medium change, an experiment was set up to compare medium change conditions. These conditions were set to full volume refreshment every 48h, 1:2 refreshment every 48h, and 1:2 refreshment every 24h.

With these conditions, after 24h of first induction, cells on 10.000 cells/cm² density plate showed polarized cell bodies, neurite formation and phase-bright perikaryon which are all morphological characteristics of neurons in a culture. While the lower density cells still had the MSC morphology as flat fibroblast like cells but with more rounded centers shown in Figure 4.2.

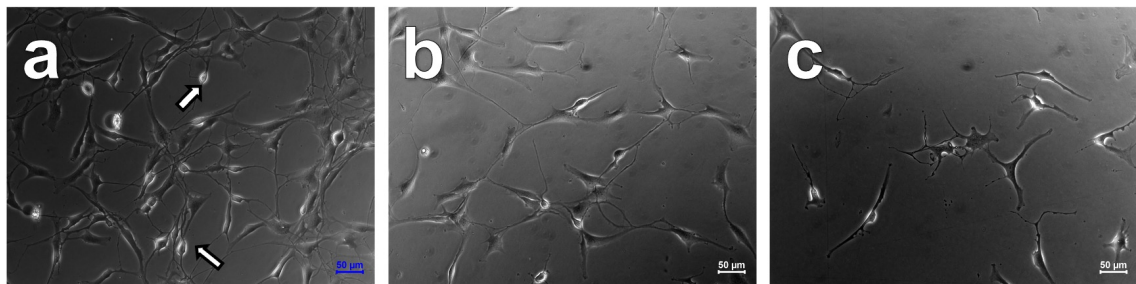


Figure 4.2 Optimal seeding density accelerates neurological morphology change. Cells seeded at (a) 10.000 cells/cm², (b) 6.000 cells/cm², (c) and 3.000 cells/cm² density after 24h of induction using single step cytokine-based neuronal differentiation medium.

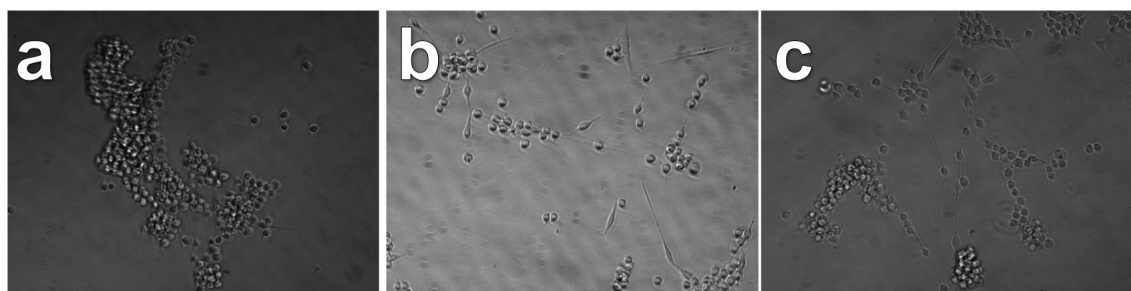


Figure 4.3 Medium change conditions affect cell death. Cells on day 4 of neuronal induction with conditions (a) complete change every 48h, (b) 1:2 change every 24h, and (c) 1:2 change every 24h.

Cells that were seeded as 10.000 cells/cm² density were compared on different medium refreshment conditions. The conditions were: full change every 48h, half

volume change every 48h and half volume change every 24h. As shown in Figure 4.3 (b) on day 4, the cells that were under 1:2 change every 48h had protected their surface adherence better than the other conditions. Preserved neutrophic factors and optimized density improved cell attachment and differentiaton.

4.2 Gelatin supports cell attachment and proliferation during neuronal differentiation.

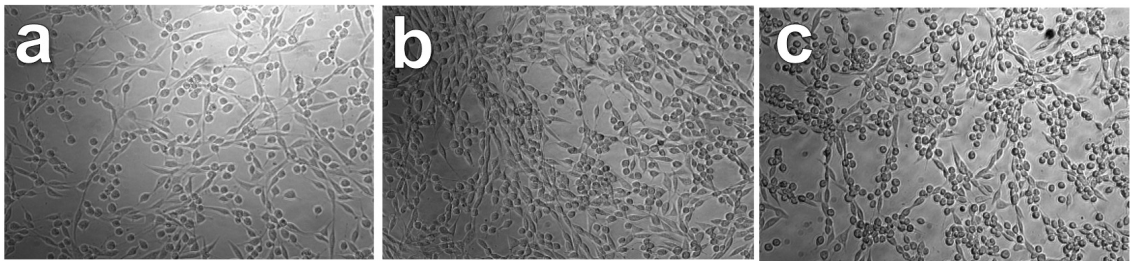


Figure 4.4 Brightfield images of MSCs on day 5 of induction on different coating materials show 0.1% gelatin coating decrease cell detachment and improve cell proliferation while collagen IV does not. (a) Differentiated cells on day 5 of induction on (a) uncoated, (b) 0.1% Gelatin coated, and (c) 10 µg/mL collagen coated plate.

Then, in order to improve cell survival and differentiation, two different coatings using extracellular matrix components were tested. Numerous studies have investigated the impact of extracellular matrix components on neuronal differentiation (Olsen, 2014), with a particular focus on gelatin and collagen (Hajiali et al., 2011). 0.1% (w/v) gelatin in 1X PBS, which is a concentration commonly used in cell culture, and 10 µg/mL collagen IV in 0.01M HCl was used for coating following the protocol previously described in section 3.2.3. Notably, cells demonstrated improved attachment on gelatin-coated surfaces, while collagen-coated surfaces did not yield the same attachment improvements. This disparity could be attributed to the specific type of neurons obtained using this method. Collagen IV, a basement membrane collagen, is predominantly found in the peripheral nervous system (Koopmans, Hasse & Sinis, 2009) and have been reported to improve neurite growth in sympathetic neurons (Lein, Higgins, Turner, Flier & Terranova, 1991).

Continuing with gelatin, to select the best gelatin concentration cells on day 4 of differentiation seeded on different concentration of coatings were analyzed for neuronal

marker MAP2 by immunostaining using the specifically optimized immunostaining protocol (3.2.5) for the neuronal differentiation experiments. 4 different concentrations were tested. Starting from 0.1% (w/v) , followed by 0.2%, and 0.4%. After applying CellProfiler's CorrectIllumination module (Figure 4.5), the objects were selected by IdentifyObjects module and the intensities were compared (Figure 4.5,(d)). The 0.2% gelatin coating had the highest intensity.

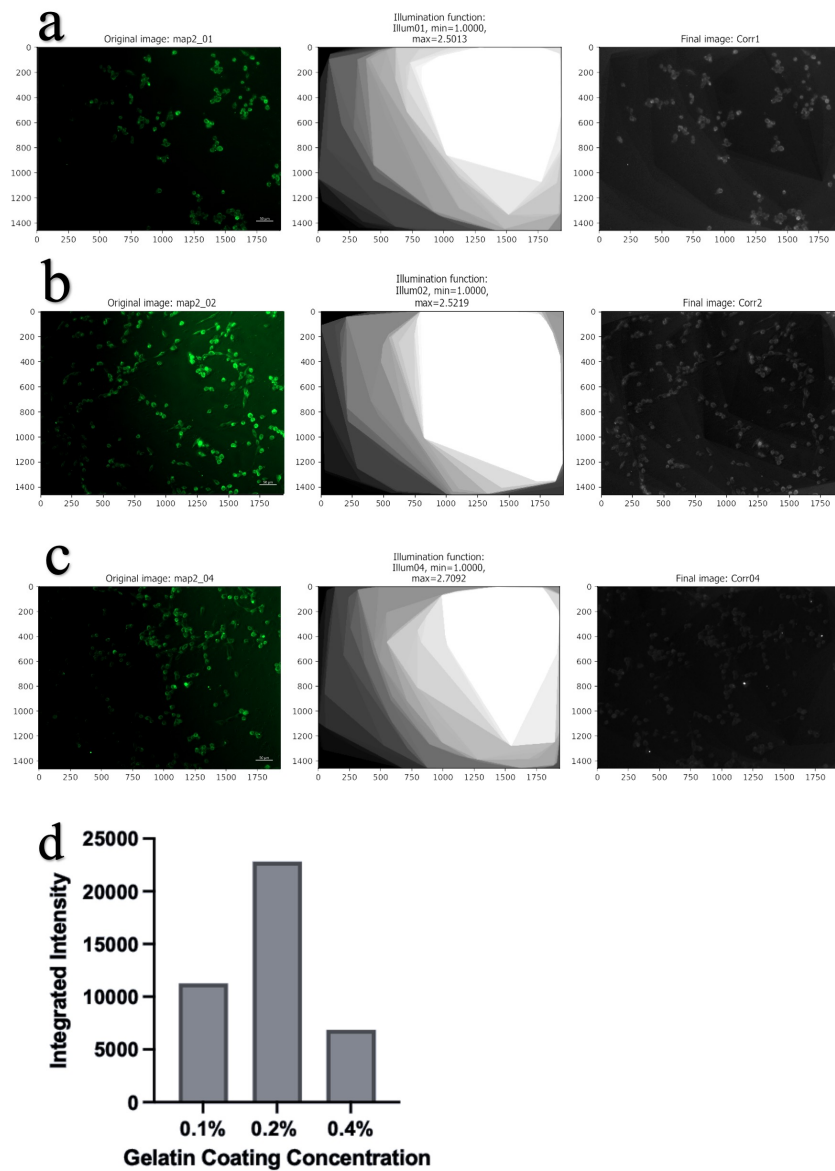


Figure 4.5 Gelatin concentration affects neuronal marker MAP2 expression. MAP2 immunostaining images processed using CellProfiler CorrectIllumination module for (a) 0.1% gelatin coating, (b) 0.2% gelatin coating, and (c) 0.4% gelatin coating. (d) IntegratedIntensity measurement comparison graph.

4.3 GNP and Gelatin Coating Affects Neuronal Marker Expression in

bm-hMSCs

hMSCs were previously reported in literature to express neuronal markers (Lindsay & Barnett, 2017). bm-hMSCs seeded at 3.000 cells/cm² density were positive for neuronal marker MAP2 and Nestin expression when immunostained according to the protocol (section 3.2.5) (Figure 4.6).

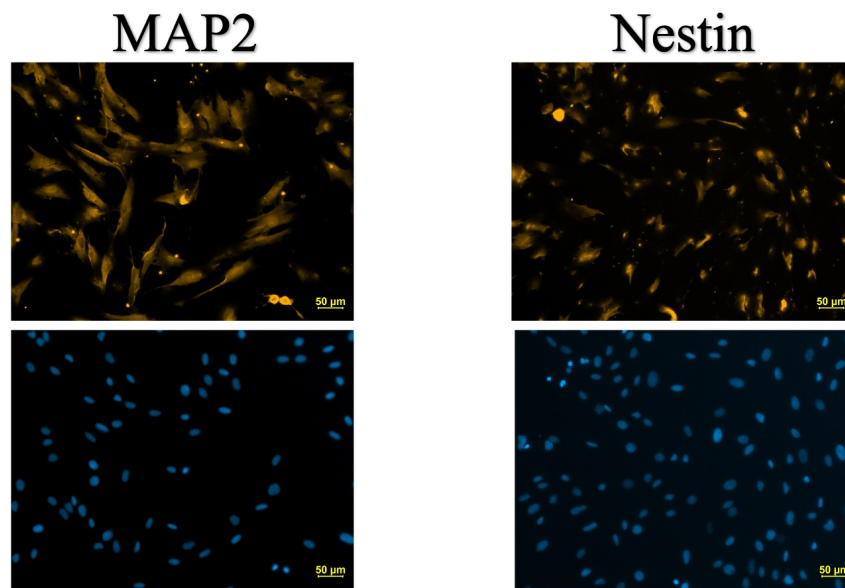


Figure 4.6 bm-hMSCs express neuronal markers MAP2 and Nestin. Fluorescent images of neuronal protein expression and DAPI staining.

Graphene oxide and other graphene products are reported to be used in neuronal differentiation to direct cells toward electro-active lineages and induce neural lineage commitment (Jin Li, 2014). However, graphene nanoplatelets' potential have not been fully discovered for this purpose. An MTT assay for a range of GNP concentration given in Figure 4.7 was performed to measure its effect on cell viability using the protocol given in methods 3.2.7. bm-hMSCs seeded on 0.1% µg/mL and 0.2% µg/mL GNP in 0.2% gelatin had the highest viability among the concentrations tested.

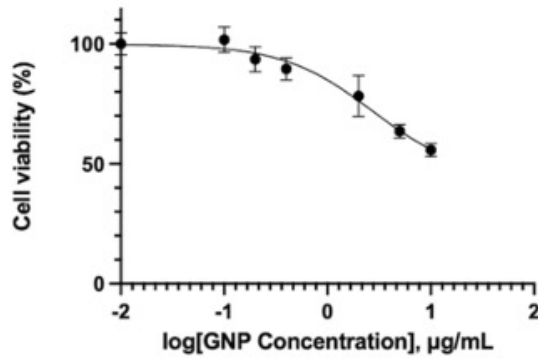


Figure 4.7 MTT cell viability assay for GNP concentrations.

To observe the effects of GNP coating and gelatin coating on marker expression in bm-hMSCs, cell culture plates were coated with 0.2 µg/mL GNP in 0.2% Gelatin prepared by thoroughly mixed GNP powder in 0.2% gelatin mixture and only 0.2% gelatin. Coating protocol was followed as given in 3.2.3. GNP coating was observed to affect the protein expression in bm-hMSCs (Figure 4.8, (b)). Unlike the other conditions which had the markers diffusely present (Figure 4.6, Figure 4.8 (a)), the conditions that had GNP coating had bright, dot appearance.

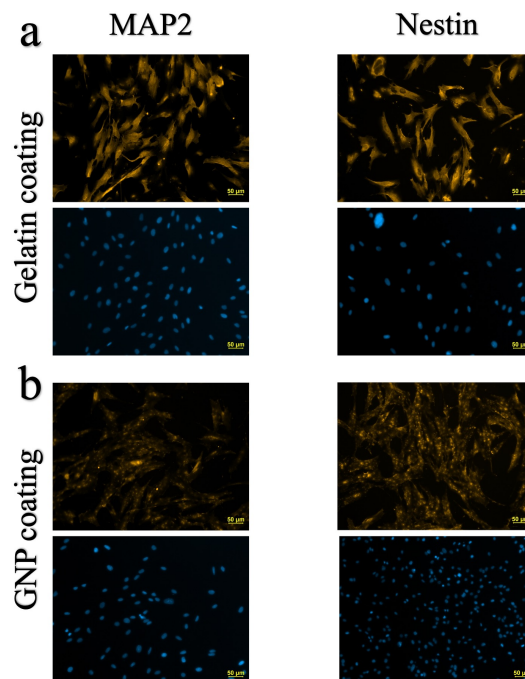


Figure 4.8 MAP2 and Nestin marker expression on bm-hMSCs with gelatin and GNP coating.

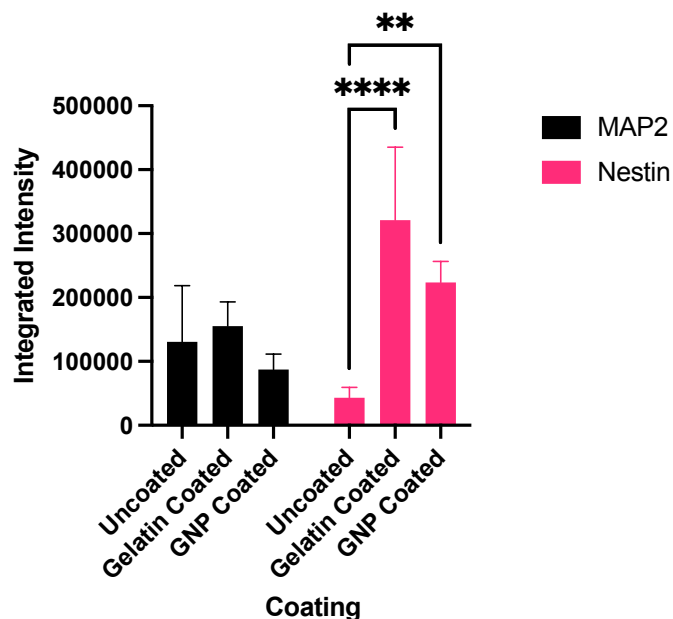


Figure 4.9 bm-hMSCs on gelatin and GNP coating shows significant increase in expression of neuronal marker Nestin. MAP2 and Nestin expression calculated by Integrated Intensity using Two-way ANOVA analysis, p value= 0,0015 and 0,0006.

On day 4 after seeding, bm-hMSCs on gelatin and 0.1 $\mu\text{g}/\text{mL}$ GNP containing gelatin expressed early neuronal marker Nestin significantly (Figure 4.9). Increase in early neuronal marker on gelatin coating shows gelatin's effect on directing bm-hMSCs into neuronal lineage commitment.

4.4 Differentiated neurons express Nestin and MAP2

On day 4 of differentiation, which is the day of differentiation when cells reach the highest differentiation percentage, differentiated neurons were positive for both Nestin (Figure 4.10) and MAP2 (Figure 4.11) neuronal markers.

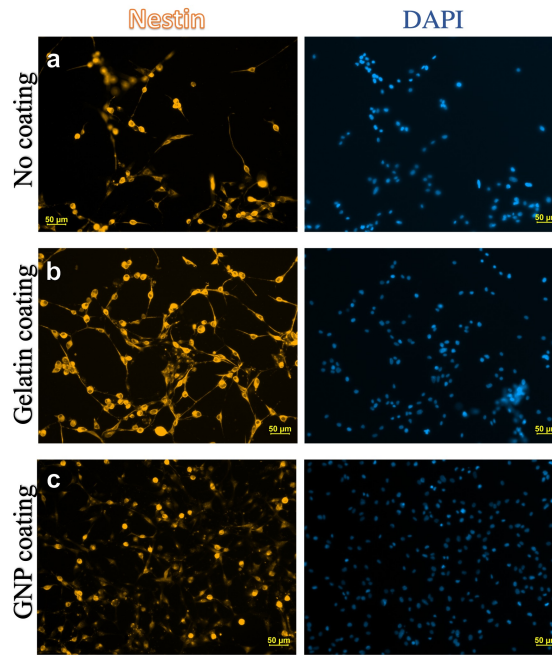


Figure 4.10 Nestin and DAPI staining for cells on day 4 of differentiation. On (a) no coating, (b) gelatin coating, and (c) GNP coating.

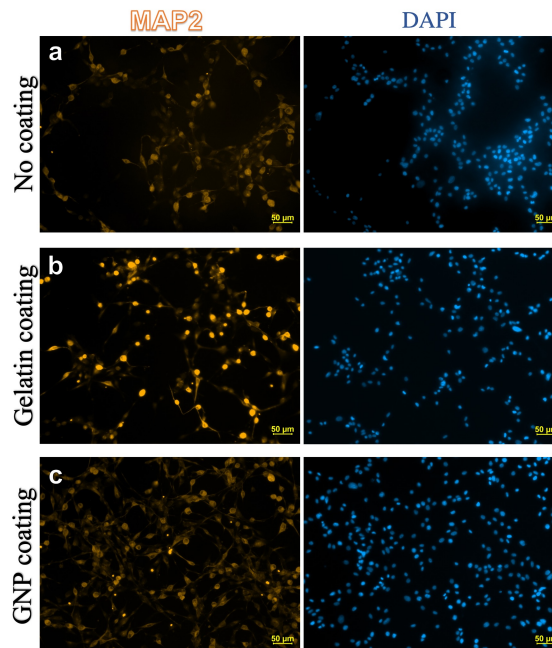


Figure 4.11 MAP2 and DAPI staining for cells on day 4 of differentiation. On (a) no coating, (b) gelatin coating, and (c) GNP coating.

Neuronal marker expression intensity then was analyzed using integrated intensity per surface area of cells. Measurements were done using CellProfiler modules "Select Primary Object", "Select Secondary Objects", "Measure Object Area" and "Measure Object Intensity". Example for the pipeline is given in Figure 4.12 (a). The Two-

way ANOVA intensity analysis did not show any significance on marker expression for different types of coating conditions (Figure 4.12(b)).

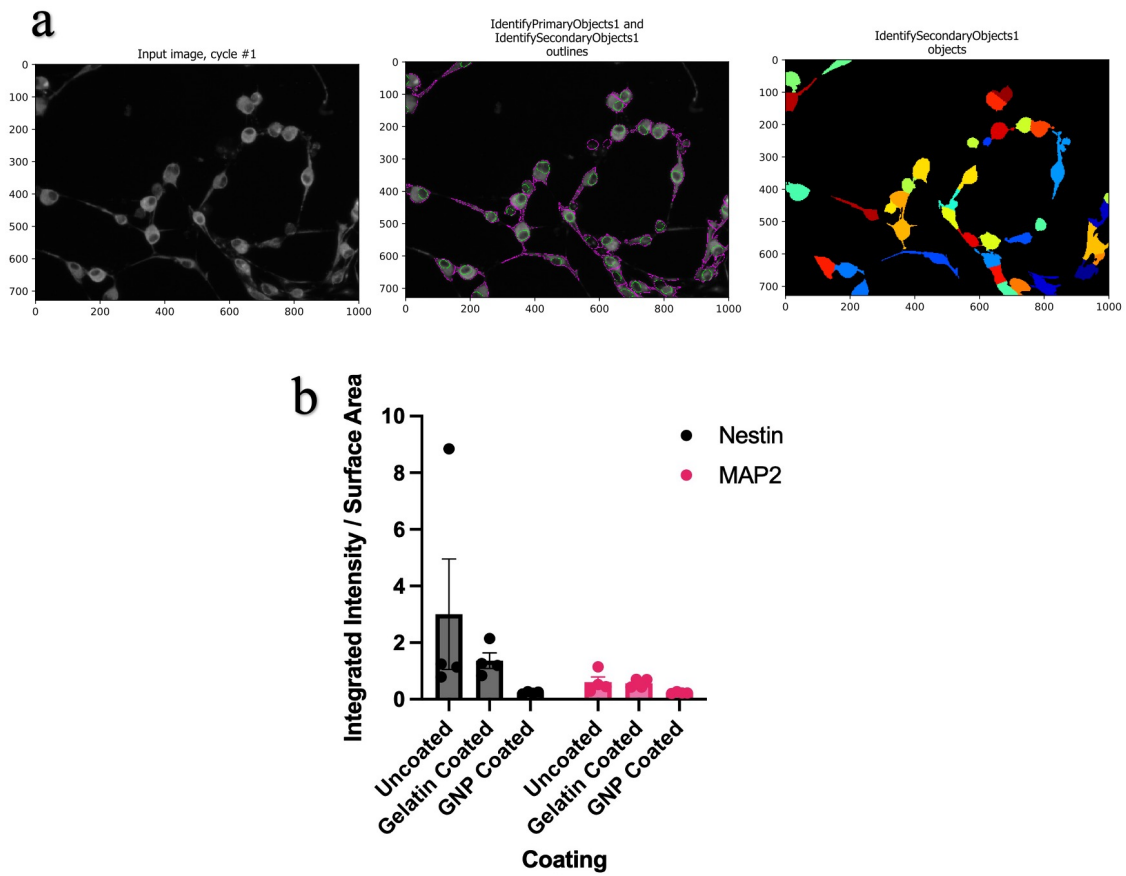


Figure 4.12 Nestin and MAP2 marker expression analysis using Integrated Intensity per surface area shows no significant difference on differentiated cells among coating conditions. (a) Representative CellProfiler Module for cell selection and analysis. (b) MAP2 and Nestin expression calculated by Integrated Intensity per surface area using Two-way ANOVA analysis.

4.5 Coating affects neuronal activity response to KCl.

Expression of neuronal markers in mesenchymal stem cells are often attributed to neuronal lineage potential or commitment. This expression does not mean that these cells acquire the functionality of mature neurons. Functioning neurons generate and propagate action potentials, form synaptic connections, and create network activity (Chanda et al., 2014). For functionality analysis of stem-cell derived neurons, recent focus has been on multi electrode arrays (MEA). MEAs record the electrical

signals generated by neurons which are then amplified, filtered, and digitized. These data can be used to evaluate response to drug treatments, network activity, seizure activity, and network phenotype.

The electrical activity of differentiated neurons was recorded using MEAs (Multi-Channel Systems, 60EcoMEA) and an MEA Reader (Kavoshgaran Electronic) on both day 4 and day 7, under various coating conditions. Seeding of bm-hMSCs and differentiation protocols were followed same as established method for cell culture plates. Depolarization was done using 15 mM KCl, which is often used for depolarization of neurons in vitro (Rienecker, Poston & Saha, 2020). Presence of KCl in the extracellular solution disrupts the electrochemical gradient due to K⁺ concentration. This disruption creates an imbalance within ion channels and transporters, forming the depolarization of neuronal membrane potential. The depolarization has the ability to trigger the opening of voltage-gated sodium channels, which in turn leads to influx of sodium ions (Na⁺), allowing further depolarization of the membrane and initiating action potentials.

Following the administration of 15 mM KCl, the neuronal activity was monitored and recorded for a duration of 5 minutes.

On day 4 of differentiation on uncoated MEA, 900 μ L 15mM KCl was introduced to the environment at 57th second. The recorded activity on electrode 6 and electrode 2 was then digitized (Figure 4.13) using the MATLAB code given in appendix. Temporal distribution of recorded individual spiking activities at a 5 KHz sampling rate presented in raster plot (Figure 4.14) showed synchronization in activity. The two electrodes located in distinct places (Figure 4.15) on the MEA surface having the synchronicity is an indication of network formation.

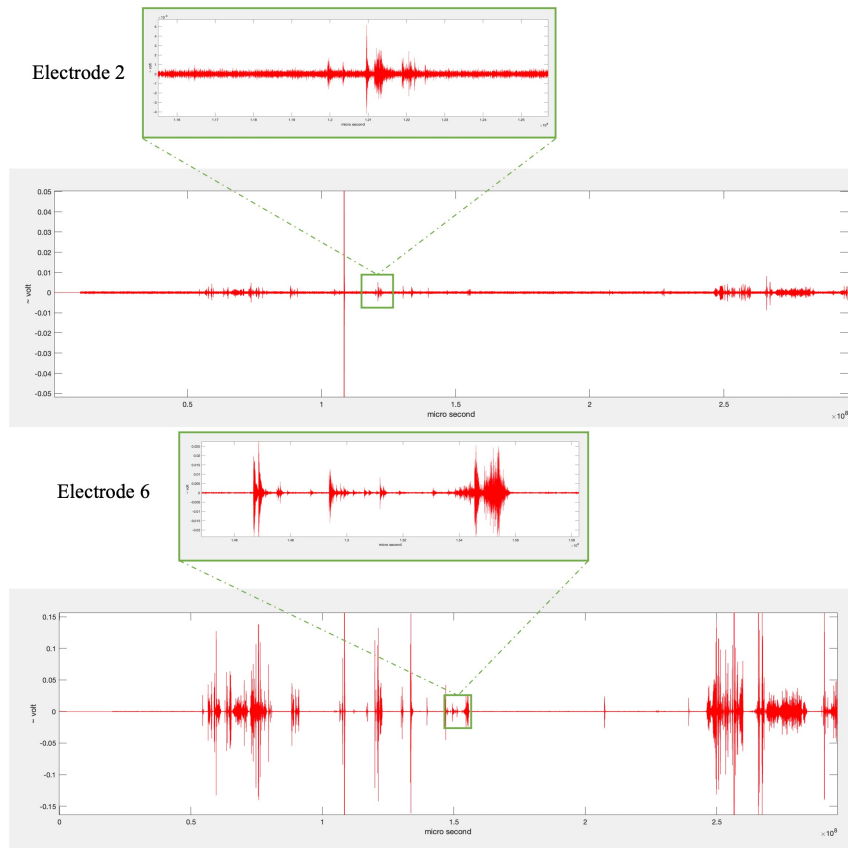


Figure 4.13 5 minutes of spiking activity on electrode 2 and electrode 6. Nerve cells at day 4 of differentiation. 15 mM KCl added at 57th second.

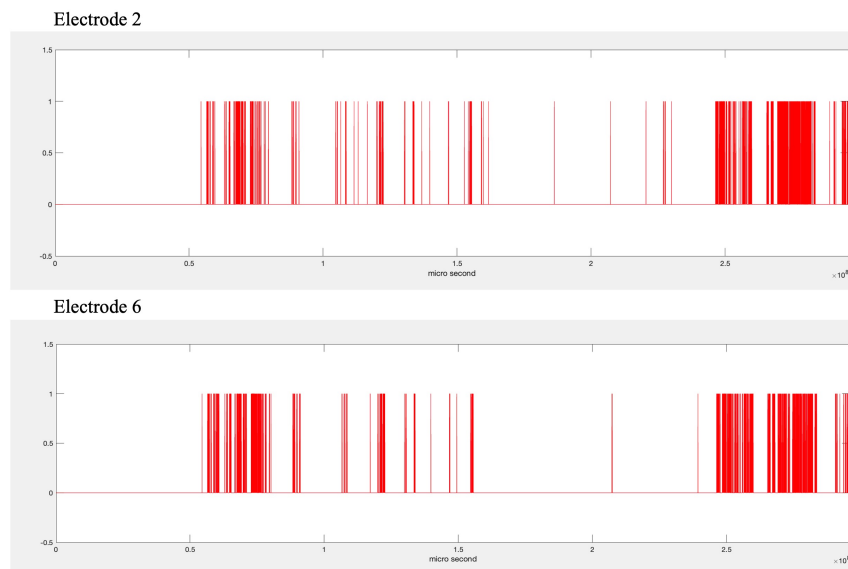


Figure 4.14 Temporal distribution of activity in raster plot for electrode 2 and electrode 6 for cells on day 4 of differentiation show synchronization. 5 KHz sampling rate.

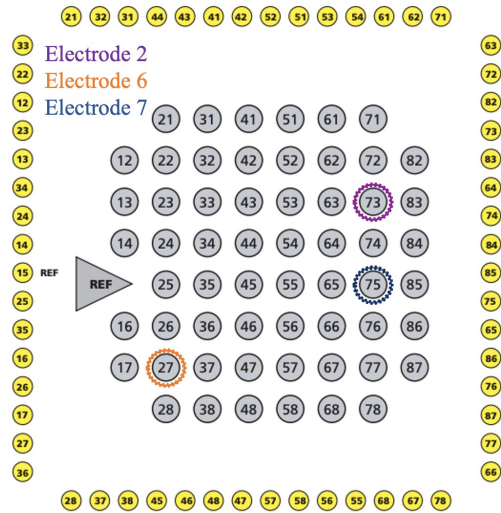


Figure 4.15 Corresponding electrode locations on the MEA surface.

On day 4 of differentiation, differentiated neurons on 0.2% gelatin coating in response to 15 mM KCl added at 43rd second have increased activity in spiking activities compared to temporal distribution of spiking activities of neurons on an uncoated MEA. (Figure 4.16)

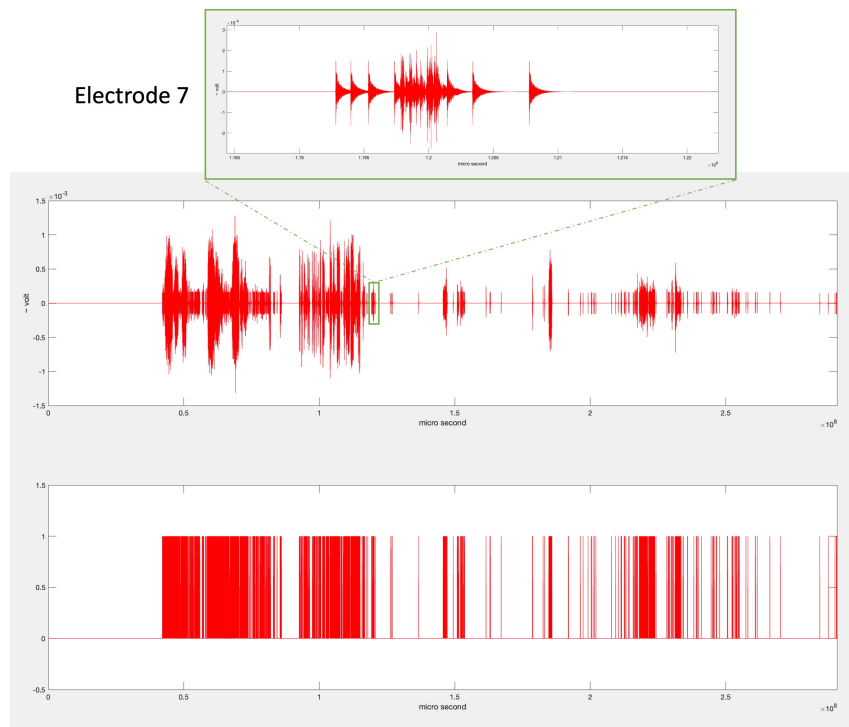


Figure 4.16 Neurons at day 4 of differentiation on a 0.2% gelatin coated MEA show increased spiking activity. 5 KHz sampling rate.

On day 7 of differentiation, which is the peak maturity day for the neurons before cell

detachment and cell death begins, both 0.2 μ g/mL GNP and 0.2% Gelatin coatings' effect on neuronal functionality was analyzed. Cells at day 7 of differentiation on GNP coating expressed a distinct temporal distribution (Figure 4.17). After 15 mM KCl treatment at 23rd second, the spiking activity started to be observed but, there is a 86,46 seconds long period where no spiking activity is observed before the activity starts again.

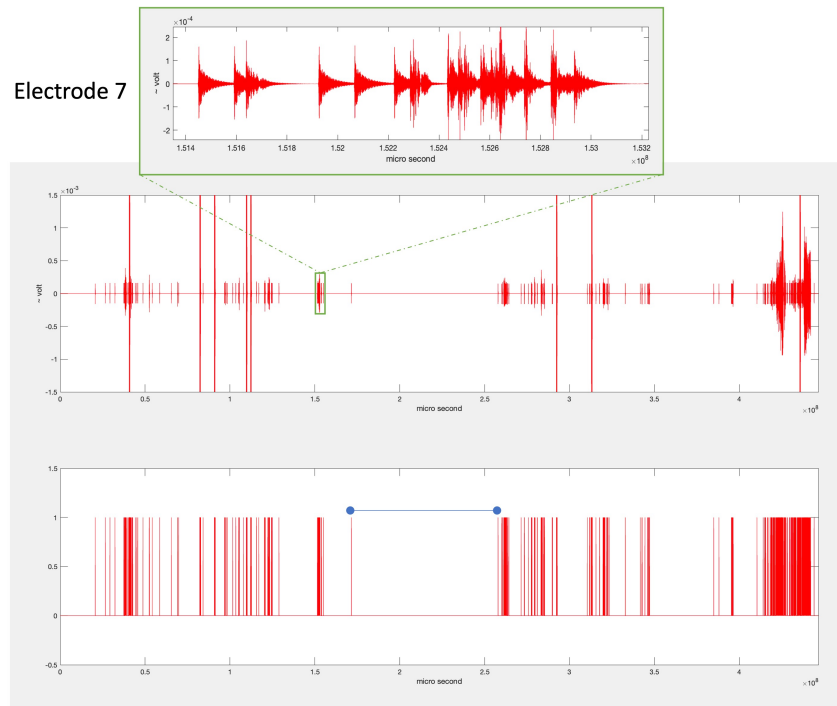


Figure 4.17 Neurons at day 7 of differentiation on a GNP coating show distinct temporal distribution in spiking activity in response to 15 mM KCl treatment. 86,46 seconds long period that records no spiking activity shown with blue line on the temporal distribution raster plot. 5 KHz sampling rate.

For the cells on day 7 of differentiation on gelatin coating, 15 mM and 30 mM KCl were used to compare neuron's response different concentrations. 15 mM KCl protocol was followed as explained previously. The recorded activity in response to 15 mM KCl treatment was then digitized. 30 mM KCl treatment was done on the same culture after 15 mM KCl treatment. 15 mM KCl solution was removed, and fresh, supplement free neurobasal medium was added to the MEA ring. Cells were incubated at 37°C, 5% CO₂ in an incubator for 30 minutes. 30 mM KCl treatment was done following the same steps to the 15 mM KCl treatment. Cells expressed increased spiking activity to 30 mM KCl treatment compared to 15 mM treatment on electrode 7 and electrode 6 (Figure 4.20).

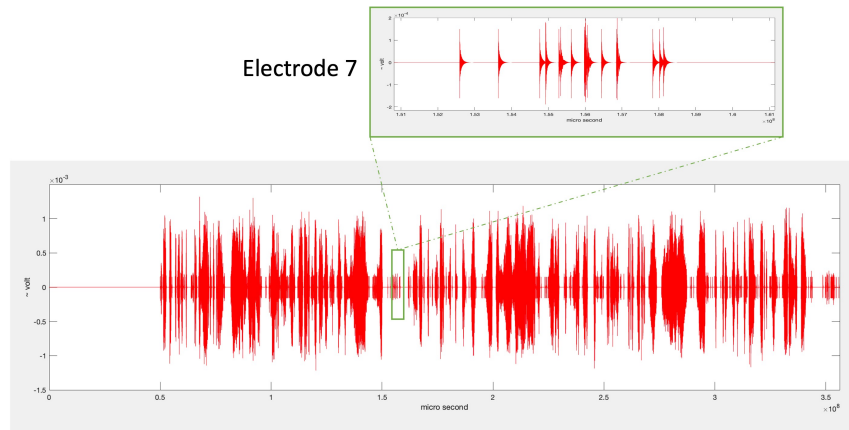


Figure 4.18 Neurons spiking activity on electrode 7 at day 7 of differentiation on 2% Gelatin coating to 15 mM KCl treatment added at 52nd second.

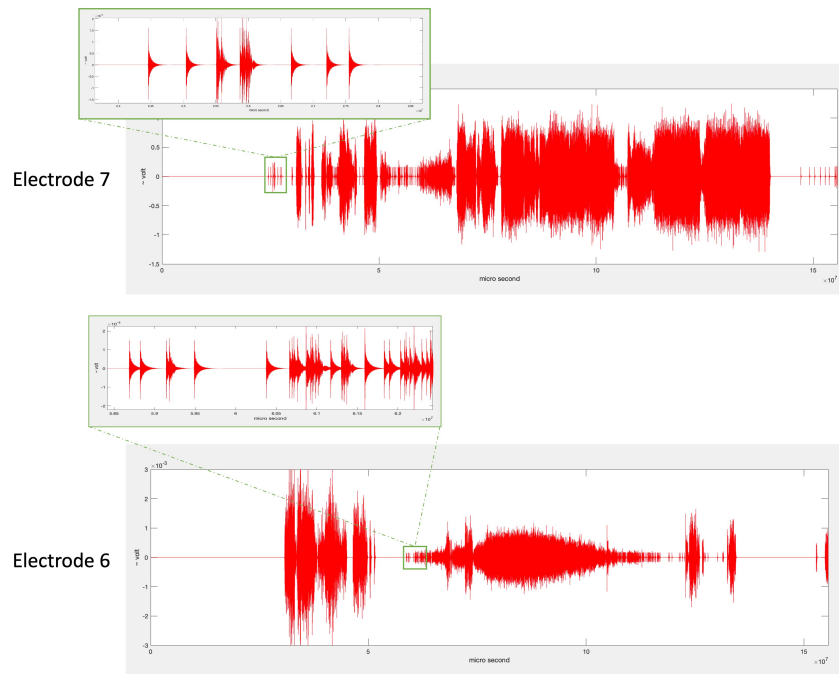


Figure 4.19 Neurons spiking activity on electrode 7 and on electrode 6 at day 7 of differentiation on 2% Gelatin coating in respons to 30 mM KCl treatment added at 30th second.

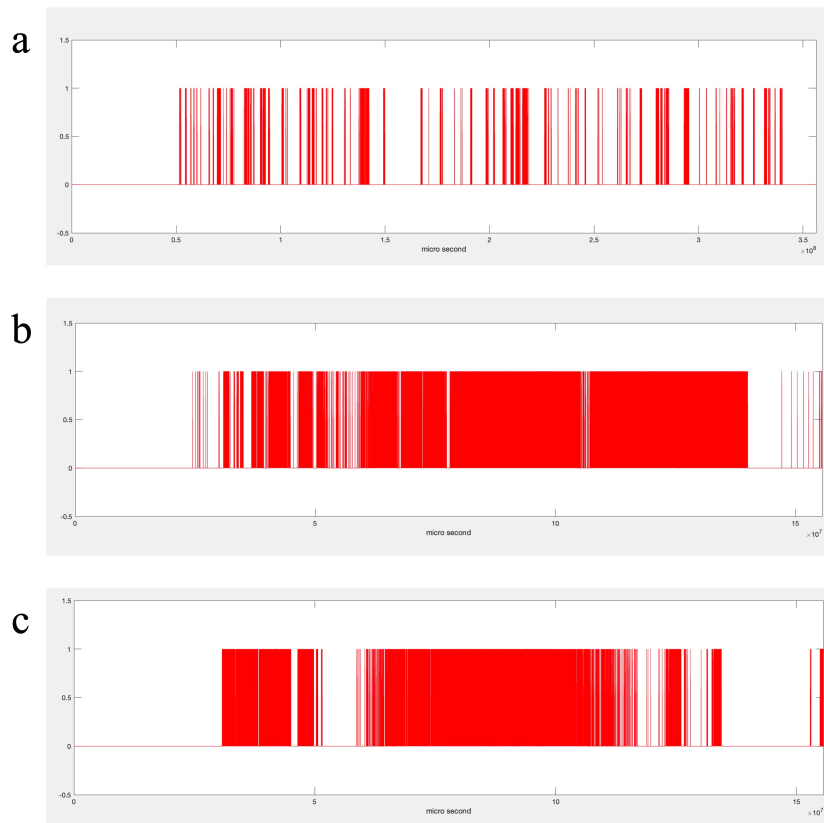


Figure 4.20 Neurons on gelatin coating at day 7 of differentiation respond to 30 mM KCl with increased spiking activity. (a) Temporal distribution of spiking activity on in response to 15 mM KCl, (b) in response to 30 mM KCl treatment on electrode 7, and (c) in response to 30 mM KCl treatment on electrode 6. Sampling rate 5 KHz.

4.6 KCl does not generate response from bm-hMSCs

In order to show the recorded spiking activity was due to depolarization of the differentiated neurons by KCl, bm-hMSCs were tested. On day 2 in culture, bm-hMSCs seeded at 10.000 cells/cm² density were dosed with 15 mM KCl. Then the recording and processing was done as previously explained. The results showed that none of the electrodes had spiking activity pattern, confirming that the recorded activity on differentiated neurons was due to depolarization of the membrane potentials. Electrode 6 has an unusual segment and Electrode 8 shows higher lines that does not correlate with spiking patterns previously observed in differentiation conditions.

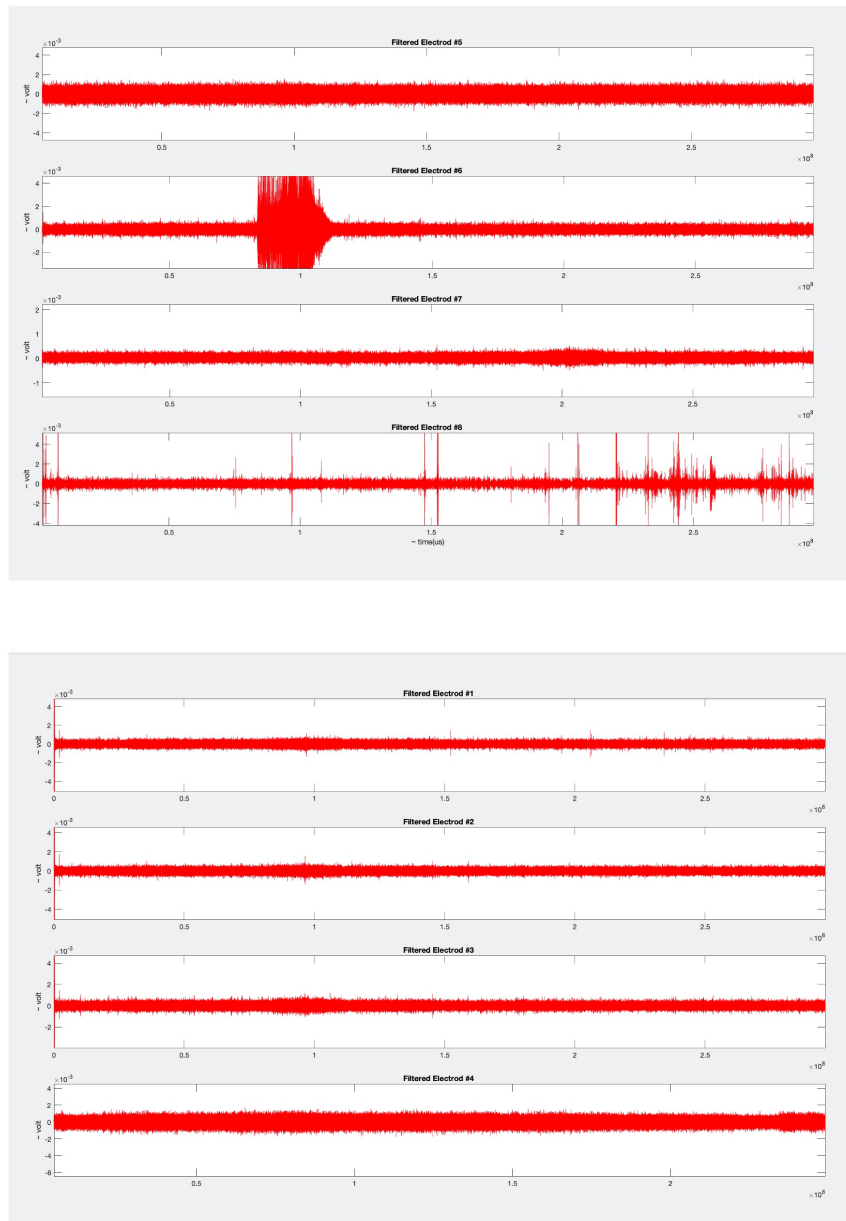


Figure 4.21 bm-hMSCs do not respond to 15 mM KCl added at the 38th second.

5. DISCUSSION

Neurological disorder studies are often hindered by limitations created by the intricate nature of the human brain and its inaccessibility for direct study. Traditional methods such as the postmortem tissue analyses and animal models often fall short in accurately recapitulating the complex mechanism of neurological disorders. This disparity creates the necessity for alternative approaches in disease modelling. Stem cell technologies, especially mesenchymal stem cells, are a promising route in addressing these challenges. MSCs can be derived from various sources, have multipotency and create low immune response. This multipotency makes them a valuable tool in studying neurological disorders. Neuronal differentiation of MSCs have been reported in multiple methods. Most common one involving the use of small molecules. Chemical inducers like cytokines and chemokines are commonly preferred method to induce the expression of specific genes that drive the differentiation of MSCs into neuronal cells.

In addition to small molecules, researchers have also been exploring the use of extracellular matrix components and triggering mechanotransduction pathways to enhance the differentiation of MSCs. The extracellular matrix provides a supportive environment for cell growth and differentiation, while mechanotransduction pathways play a role in cellular responses to mechanical forces. MSCs respond to soft matrices by increased activation and internalization of integrins. Stiffer matrices cause integrins to localize on the cell surface. Internalization of By manipulating the mechanical and chemical properties of the materials, researchers aim to improve the efficiency and effectiveness of neuronal differentiation of MSCs. Overall, stem cell technology, particularly the use of MSCs, coupled with use of ECM offers a promising approach to overcome the limitations of traditional methods in studying neurological disorders.

Karakaş et al. (2020) described a neuronal differentiation medium used for human bone-marrow derived MSCs. The neurons obtained through this method were reported to be cultured up to 21 days and exhibited spontaneous activity which was demonstrated by Ca^{++} imaging. Within 24 hours, the differentiation medium in-

duced morphological changes in the cells, including polarized cell bodies, neurite formation, and phase-bright perikaryon. However, after 4 days in culture, the cells detached from the culture plate and underwent cell death.

Cells' total day in culture was improved to 8 days from 4 through cell culture condition improvements and use of extracellular matrix components. Optimized seeding density and medium refreshment conditions can improve cell survival due to preserved neurotrophic factors secreted by the MSCs (Wilkins et al., 2009) and decreased excitotoxicity (Anilkumar et al., 2017).

Matrix stiffness and chemical composition affects mechanotransduction cascades of MSCs which results in either increased proliferation and/or differentiation. Numerous studies have investigated the impact of extracellular matrix components on neuronal differentiation (Olsen, 2014), with a particular focus on gelatin and collagen (Hajiali et al., 2011). Gelatin is a polymer derived from partial hydrolysis of collagen, containing integrin binding sites which aids cell adhesion, migration and differentiation.

Our results have shown that 0.2% gelatin coating and 0.2 μ g/mL GNP coating increase early neuronal marker Nestin significantly on bm-hMSCs after 4 days in culture.

For neuronal differentiation protocols, due to their origins, dental-tissue derived MSCs can be the initial focus (Kim, Lee, Xu, Zhang & Le, 2021). Dental-tissue derived MSCs originate from the neural crest cells, which are responsible for generating neurons and glial cells of the peripheral nervous system. However, bm-hMSCs have also been reported to express neuronal markers NeuN, Nestin and MAP2 in the literature. Furthermore, human bm-MSCs were found to express neuronal markers β III-tubulin and Neun regardless of passage and culture conditions, or even after osteogenic and adipogenic differentiation (Foudah, Redondo, Caldara, Carini, Tredici & Miloso, 2013). In fact, Morikawa, Mabuchi, Niibe, Suzuki, Nagoshi, Sunabori, Shimmura, Nagai, Nakagawa, Okano & others (2009) detected MSCs that originate from neural crest in a bone-marrow derived MSC culture. This finding suggest that even though a MSC population is derived from mesoderm, it can contain cells that have origins from development of cells that create peripheral nervous system. These aforementioned findings also can be interpreted as that neuronal marker expression alone is not sufficient to assess a neuronal differentiation protocol. Increased Nestin marker expression in bm-hMSCs on gelatin coating could be attributed to neuronal lineage commitment which does not necessarily mean a neuronal differentiation as they still have MSC morphology.

Functionality assessment of stem-cell derived neurons is crucial for several reasons. Firstly, it is important to determine that the differentiation protocol can yield cells that can capture distinctive properties of a neuron. Neurons respond to stimuli by generating and propagating action potentials, form synaptic connections that create network activity through synaptic connections (Chanda et al., 2014). Secondly, functional analysis of stem-cell derived neurons can give valuable insight in disease modelling applications. CNS disorders and diseases exhibit unique neuronal conditions that needs accurate representation in a model. Measurement and analysis of functionality of a stem-cell derived neuron culture allows selection of the right type of neuron for the specific intended purpose. Multielectrode arrays (MEAs) can provide the needed functionality analysis by detecting generated action potentials from individual neurons on a culture. MEAs have been used in vivo for decades and are now being used in vitro studies. Most studies that employ MEAs with neurons in 2D cultures use neurons derived from hiPSCs. Through comparison with in vivo recordings of MEAs and EEGs, there has been a cumulation of knowledge built to close the gap between the human brain studies and in vitro studies. hiPSC derived neurons have been used to study a variety of topics from physiology of these cells to creating pathological conditions. The type of neuron and network dynamics are being identified through this data. In addition to these, by exposing the neuronal network to compounds, drug response and therefore potential treatments can be investigated. These studies will close the gap between the models and the human brain that is currently is either left open or filled by animal studies. Here, we have used an MEA (MultiChannel Systems, 60EcoME) to analyze spiking activity of neurons under various conditions of neuronal differentiation protocol. Firstly, neuronal cells on day 4 were exposed to 15 mM KCl. This KCl exposure induces neurons to get depolarized, leading to generation of action potentials. The neurons on day 4 of differentiation expressed depolarization activity which indicates their functionality. The recording on two electrode locations demonstrated synchronization that is interpreted as a sign of network formation (Shin, Jeong, Lee, Sun, Choi & Cho, 2021). According to Shin et al. (2021) findings, the number of synaptic connections increase in a culture as the network formation progresses which in return increases the synchronized electrode numbers and burst activity among neurons. For our differentiation protocol, an increase in both these values for coating conditions was anticipated. On day 4 of differentiation, neurons on gelatin coating indeed had greater number of spiking activity in response to KCl treatment. Supporting the progressed neuronal network by more days in culture findings, on day 7 of differentiation, neurons seeded on gelatin coating exhibit the highest number of spikes compared to all 15 mM KCl treatments. However, using the data from multiple electrodes to asses the synchronization was not possible. This could be due to reusable MEAs getting

harmed during sterilization procedures or due to loss of synaptic connections before cells completely detach and die on day 8. The differentiation and spiking activity was supported with the experiment using undifferentiated bm-hMSCs. bm-hMSCs seeded at 10,000 cells/cm² were introduced to 15 mM KCl on day 2 in culture. Across the electrodes, there was not any spiking activity observed that matches the patterns observed on differentiated neurons. However, on electrode 6, there was a high noise-like activity which was not observed before. And, on electrode 8, there are high recording lines but these lines do not create the spiking pattern that was observed on differentiation recordings.

Graphene nanoplatelets were another ECM component that were used to enhance the neuronal differentiation in this thesis. Graphene and graphene oxide products have been integrated to scaffolds and surfaces in differentiation protocols due to their properties such as electrical conductivity, thermal conductivity and mechanical strength. Especially graphene oxide and reduced graphene oxide which can be functionalized or show higher electrical conductivity. The electrical conductivity of the material was thought to be a striking factor in directing stem cells into committing electrically active lineages such as neurons. However, graphene nanoplatelets' potential in this area has not been discovered. Graphene nanoplatelets are a graphene product obtained from exfoliation of graphite. And by adding these nanoplatelets into gelatin coating, graphene nanoplatelet coating was obtained. This graphene nanoplatelet coating was expected to increase spiking activity due to its properties attributed to graphene products. However, neurons on GNP coating showed a distinct pattern where it has a 86,46 seconds halt between recurring activity periods. This period could have suppressed activity that was filtered during data processing. In a study done with MEAs located on neocortex of 4 epilepsy patients, it was reported that there was a cease of spiking activity between seizures (Trucolo, Donoghue, Hochberg, Eskandar, Madsen, Anderson, Brown, Halgren & Cash, 2011). There are periods on other recordings with low to no activity as well. However, these periods are always led and followed by frequent activity. So, this firing behavior is different than other conditions and it requires more in depth analysis to provide insight. Another experiment condition was done to compare response to increased KCl concentration. Conducting this comparison supports the confidence that neurons have dose-dependent activity when moving forward to future aspects of this protocol where it can be employed in disease modelling and drug testing. And as expected, the differentiated neurons responded by increased spiking activity to increased KCl concentrations.

Overall, this optimized protocol provides neurons differentiated from bm-hMSCs to last longer in culture and have higher functionality shown by recordings done using

MEAs. Whilst 2D cultures of neurons are less complicated and do not fully represent the complexity of the human brain, application of MEAS into microfluidic devices is a promising and exciting destination for the future. Together with microfluidic device technology, MEAs can provide insight to neuronal activity in disease conditions, blood brain barrier interactions and overall neuronal behavior.

BIBLIOGRAPHY

- Adani, B., Basheer, M., Hailu, A. L., Fogel, T., Israeli, E., Volinsky, E., & Gorodetsky, R. (2019). Isolation and expansion of high yield of pure mesenchymal stromal cells from fresh and cryopreserved placental tissues. *Cryobiology*, *89*, 100–103.
- Ahmadvand, T., Mirsadeghi, S., Shanehsazzadeh, F., Kiani, S., & Fardmanesh, M. (2020). A novel low-cost method for fabrication of 2d multi-electrode array (mea) to evaluate functionality of neuronal cells. In *Proceedings*, volume 60, (pp.51). MDPI.
- Anilkumar, U., Weisova, P., Schmid, J., Bernas, T., Huber, H. J., Düssmann, H., Connolly, N. M., & Prehn, J. H. (2017). Defining external factors that determine neuronal survival, apoptosis and necrosis during excitotoxic injury using a high content screening imaging platform. *PLoS One*, *12*(11), e0188343.
- Aust, L., Devlin, B., Foster, S., Halvorsen, Y., Hicok, K., Du Laney, T., Sen, A., Willingmyre, G., & Gimble, J. (2004). Yield of human adipose-derived adult stem cells from liposuction aspirates. *Cytotherapy*, *6*(1), 7–14.
- Baksh, D., Davies, J. E., & Zandstra, P. W. (2003). Adult human bone marrow-derived mesenchymal progenitor cells are capable of adhesion-independent survival and expansion. *Experimental hematology*, *31*(8), 723–732.
- Berk, C. & Sabbagh, M. N. (2013). Successes and failures for drugs in late-stage development for alzheimer’s disease. *Drugs & aging*, *30*, 783–792.
- Borkowska, P., Kowalska, J., Fila-Danilow, A., Bielecka, A. M., Paul-Samojedny, M., Kowalczyk, M., & Kowalski, J. (2015). Affect of antidepressants on the in vitro differentiation of rat bone marrow mesenchymal stem cells into neuronal cells. *European Journal of Pharmaceutical Sciences*, *73*, 81–87.
- Buzsáki, G., Anastassiou, C. A., & Koch, C. (2012). The origin of extracellular fields and currents—eeg, ecog, lfp and spikes. *Nature reviews neuroscience*, *13*(6), 407–420.
- Cecchelli, R., Berezowski, V., Lundquist, S., Culot, M., Renftel, M., Dehouck, M.-P., & Fenart, L. (2007). Modelling of the blood–brain barrier in drug discovery and development. *Nature reviews Drug discovery*, *6*(8), 650–661.
- Chanda, S., Ang, C. E., Davila, J., Pak, C., Mall, M., Lee, Q. Y., Ahlenius, H., Jung, S. W., Südhof, T. C., & Wernig, M. (2014). Generation of induced neuronal cells by the single reprogramming factor ascl1. *Stem cell reports*, *3*(2), 282–296.
- Colter, D. C., Class, R., DiGirolamo, C. M., & Prockop, D. J. (2000). Rapid expansion of recycling stem cells in cultures of plastic-adherent cells from human bone marrow. *Proceedings of the National Academy of Sciences*, *97*(7), 3213–3218.
- De Los Angeles, A., Ferrari, F., Xi, R., Fujiwara, Y., Benvenisty, N., Deng, H., Hochedlinger, K., Jaenisch, R., Lee, S., Leitch, H. G., et al. (2015). Hallmarks of pluripotency. *Nature*, *525*(7570), 469–478.
- Dominici, M., Le Blanc, K., Mueller, I., Slaper-Cortenbach, I., Marini, F., Krause, D., Deans, R., Keating, A., Prockop, D., & Horwitz, E. (2006). Minimal criteria for defining multipotent mesenchymal stromal cells. the international

- society for cellular therapy position statement. *Cytotherapy*, 8(4), 315–317.
- Engler, A. J., Sen, S., Sweeney, H. L., & Discher, D. E. (2006). Matrix elasticity directs stem cell lineage specification. *Cell*, 126(4), 677–689.
- Feigin, V. L. (2019). Global, regional, and national burden of neurological disorders, 1990–2016: a systematic analysis for the global burden of disease study 2016. *The Lancet Neurology*, 18(5), 459–480.
- Ferrari, G., Cusella, G., Angelis, D., Coletta, M., Paolucci, E., Stornaiuolo, A., Cossu, G., & Mavilio, F. (1998). Muscle regeneration by bone marrow-derived myogenic progenitors. *Science*, 279(5356), 1528–1530.
- Fonsatti, E., Sigalotti, L., Arslan, P., Altomonte, M., & Maio, M. (2003). Emerging role of endoglin (cd105) as a marker of angiogenesis with clinical potential in human malignancies. *Current Cancer Drug Targets*, 3(6), 427–432.
- Foudah, D., Redondo, J., Caldara, C., Carini, F., Tredici, G., & Miloso, M. (2013). Human mesenchymal stem cells express neuronal markers after osteogenic and adipogenic differentiation. *Cellular and Molecular Biology Letters*, 18(2), 163–186.
- Gordon, P. H. & Meininger, V. (2011). How can we improve clinical trials in amyotrophic lateral sclerosis? *Nature Reviews Neurology*, 7(11), 650.
- Gribkoff, V. K. & Kaczmarek, L. K. (2017). The need for new approaches in cns drug discovery: Why drugs have failed, and what can be done to improve outcomes. *Neuropharmacology*, 120, 11–19. Beyond Small Molecules for Neurological Disorders.
- Grienberger, C. & Konnerth, A. (2012). Imaging calcium in neurons. *Neuron*, 73(5), 862–885.
- Hajiali, H., Shahgasempour, S., Naimi-Jamal, M. R., & Peirovi, H. (2011). Electrospun pga/gelatin nanofibrous scaffolds and their potential application in vascular tissue engineering. *International journal of nanomedicine*, 2133–2141.
- Harris, K. D., Quiroga, R. Q., Freeman, J., & Smith, S. L. (2016). Improving data quality in neuronal population recordings. *Nature neuroscience*, 19(9), 1165–1174.
- Hernández, R., Jiménez-Luna, C., Perales-Adán, J., Perazzoli, G., Melguizo, C., & Prados, J. (2020). Differentiation of human mesenchymal stem cells towards neuronal lineage: clinical trials in nervous system disorders. *Biomolecules & therapeutics*, 28(1), 34.
- Huber, J. D., Egleton, R. D., & Davis, T. P. (2001). Molecular physiology and pathophysiology of tight junctions in the blood-brain barrier. *Trends in Neurosciences*, 24(12), 719–725.
- Hurko, O. & Ryan, J. L. (2005). Translational research in central nervous system drug discovery. *NeuroRx*, 2(4), 671–682.
- Jones, E. A., Kinsey, S. E., English, A., Jones, R. A., Straszynski, L., Meredith, D. M., Markham, A. F., Jack, A., Emery, P., & McGonagle, D. (2002a). Isolation and characterization of bone marrow multipotential mesenchymal progenitor cells. *Arthritis & Rheumatism*, 46(12), 3349–3360.
- Jones, E. A., Kinsey, S. E., English, A., Jones, R. A., Straszynski, L., Meredith, D. M., Markham, A. F., Jack, A., Emery, P., & McGonagle, D. (2002b). Isolation and characterization of bone marrow multipotential mesenchymal progenitor cells. *Arthritis & Rheumatism*, 46(12), 3349–3360.
- Kaminska, A., Radoszkiewicz, K., Rybkowska, P., Wedzinska, A., & Sarnowska, A.

- (2022). Interaction of neural stem cells (nsCs) and mesenchymal stem cells (msCs) as a promising approach in brain study and nerve regeneration. *Cells*, *11*(9), 1464.
- Kamioka, H., Maeda, E., Jimbo, Y., Robinson, H. P., & Kawana, A. (1996). Spontaneous periodic synchronized bursting during formation of mature patterns of connections in cortical cultures. *Neuroscience letters*, *206*(2-3), 109–112.
- Karakaş, N., Bay, S., Türkel, N., Öztunç, N., Öncül, M., Bilgen, H., Shah, K., Şahin, F., & Öztürk, G. (2020). Neurons from human mesenchymal stem cells display both spontaneous and stimuli responsive activity. *PLoS One*, *15*(5), e0228510.
- Karaöz, E., Doğan, B. N., Aksoy, A., Gacar, G., Akyüz, S., Ayhan, S., Genç, Z. S., Yürüker, S., Duruksu, G., Demircan, P. Ç., et al. (2010). Isolation and in vitro characterisation of dental pulp stem cells from natal teeth. *Histochemistry and cell biology*, *133*, 95–112.
- Kim, D., Lee, A. E., Xu, Q., Zhang, Q., & Le, A. D. (2021). Gingiva-derived mesenchymal stem cells: potential application in tissue engineering and regenerative medicine—a comprehensive review. *Frontiers in Immunology*, *12*, 667221.
- Kizner, V., Fischer, S., & Naujock, M. (2019). Multielectrode array (mea)-based detection of spontaneous network activity in human ipsc-derived cortical neurons. *Cell-Based Assays Using iPSCs for Drug Development and Testing*, 209–216.
- Koopmans, G., Hasse, B., & Sinis, N. (2009). The role of collagen in peripheral nerve repair. *International review of neurobiology*, *87*, 363–379.
- Kuznetsov, S. A., Friedenstein, A. J., & Gehron Robey, P. (1997). Factors required for bone marrow stromal fibroblast colony formation in vitro. *British Journal of Haematology*, *97*(3), 561–570.
- Lambert, C., Preijers, F. W., Yanikkaya Demirel, G., & Sack, U. (2017). Monocytes and macrophages in flow: an escca initiative on advanced analyses of monocyte lineage using flow cytometry.
- Lee, Y.-J., Seo, T. H., Lee, S., Jang, W., Kim, M. J., & Sung, J.-S. (2018). Neuronal differentiation of human mesenchymal stem cells in response to the domain size of graphene substrates. *Journal of Biomedical Materials Research Part A*, *106*(1), 43–51.
- Lein, P. J., Higgins, D., Turner, D. C., Flier, L. A., & Terranova, V. P. (1991). The nc1 domain of type iv collagen promotes axonal growth in sympathetic neurons through interaction with the alpha 1 beta 1 integrin. *The Journal of cell biology*, *113*(2), 417–428.
- Li, X., Zhang, Y., & Qi, G. (2013). Evaluation of isolation methods and culture conditions for rat bone marrow mesenchymal stem cells. *Cytotechnology*, *65*, 323–334.
- Lim, K.-T., Seonwoo, H., Choi, K. S., Jin, H., Jang, K.-J., Kim, J., Kim, J.-W., Kim, S. Y., Choung, P.-H., & Chung, J. H. (2016). Pulsed-electromagnetic-field-assisted reduced graphene oxide substrates for multidifferentiation of human mesenchymal stem cells. *Advanced healthcare materials*, *5*(16), 2069–2079.
- Lindsay, S. L. & Barnett, S. C. (2017). Are nestin-positive mesenchymal stromal cells a better source of cells for CNS repair? *Neurochemistry international*, *106*, 101–107.

- Little, D., Ketteler, R., Gissen, P., & Devine, M. J. (2019). Using stem cell-derived neurons in drug screening for neurological diseases. *Neurobiology of Aging*, *78*, 130–141.
- Marg, E. & Adams, J. E. (1967). Indwelling multiple micro-electrodes in the brain. *Electroencephalography and clinical neurophysiology*, *23*(3), 277–280.
- Mason, W. P. (2015). Blood-brain barrier-associated efflux transporters: a significant but underappreciated obstacle to drug development in glioblastoma. *Neuro-Oncology*, *17*(9), 1181.
- Medberry, C. J., Crapo, P. M., Siu, B. F., Carruthers, C. A., Wolf, M. T., Nagarkar, S. P., Agrawal, V., Jones, K. E., Kelly, J., Johnson, S. A., et al. (2013). Hydrogels derived from central nervous system extracellular matrix. *Biomaterials*, *34*(4), 1033–1040.
- Méndez-Ferrer, S., Michurina, T. V., Ferraro, F., Mazloom, A. R., MacArthur, B. D., Lira, S. A., Scadden, D. T., Ma'ayan, A., Enikolopov, G. N., & Frenette, P. S. (2010). Mesenchymal and haematopoietic stem cells form a unique bone marrow niche. *nature*, *466*(7308), 829–834.
- Morikawa, S., Mabuchi, Y., Niibe, K., Suzuki, S., Nagoshi, N., Sunabori, T., Shimura, S., Nagai, Y., Nakagawa, T., Okano, H., et al. (2009). Development of mesenchymal stem cells partially originate from the neural crest. *Biochemical and biophysical research communications*, *379*(4), 1114–1119.
- Nakagawa, S. (2010). Involvement of neurogenesis in the action of psychotropic drugs. *Nihon Shinkei Seishin Yakurigaku Zasshi= Japanese Journal of Psychopharmacology*, *30*(3), 109–113.
- Nakano, A., Harada, T., Morikawa, S., & Kato, Y. (1990). Expression of leukocyte common antigen (cd45) on various human leukemia/lymphoma cell lines. *Pathology International*, *40*(2), 107–115.
- Novoselov, K. S., Geim, A. K., Morozov, S. V., Jiang, D.-e., Zhang, Y., Dubonos, S. V., Grigorieva, I. V., & Firsov, A. A. (2004). Electric field effect in atomically thin carbon films. *science*, *306*(5696), 666–669.
- Olsen, B. R. (2014). Matrix molecules and their ligands. In *Principles of tissue engineering* (pp. 189–208). Elsevier.
- Park, S. Y., Park, J., Sim, S. H., Sung, M. G., Kim, K. S., Hong, B. H., & Hong, S. (2011). Enhanced differentiation of human neural stem cells into neurons on graphene. *Advanced materials*, *23*(36), H263–H267.
- Patel, M., Moon, H. J., Ko, D. Y., & Jeong, B. (2016). Composite system of graphene oxide and polypeptide thermogel as an injectable 3d scaffold for adipogenic differentiation of tonsil-derived mesenchymal stem cells. *ACS Applied Materials & Interfaces*, *8*(8), 5160–5169.
- Patwari, P. & Lee, R. T. (2008). Mechanical control of tissue morphogenesis. *Circulation research*, *103*(3), 234–243.
- Pelkonen, A., Pistono, C., Klecki, P., Gómez-Budia, M., Dougalis, A., Konttinen, H., Stanová, I., Fagerlund, I., Leinonen, V., Korhonen, P., et al. (2021). Functional characterization of human pluripotent stem cell-derived models of the brain with microelectrode arrays. *Cells*, *11*(1), 106.
- Peng, C. & Zhang, X. (2021). Chemical functionalization of graphene nanoplatelets with hydroxyl, amino, and carboxylic terminal groups. *Chemistry*, *3*(3), 873–888.
- Piccolo, F., Battiato, A., Bernardi, E., Plaitano, M., Franchino, C., Gosso, S.,

- Pasquarelli, A., Carbone, E., Olivero, P., & Carabelli, V. (2016). All-carbon multi-electrode array for real-time in vitro measurements of oxidizable neurotransmitters. *Scientific reports*, *6*(1), 20682.
- Pittenger, M. F., Mackay, A. M., Beck, S. C., Jaiswal, R. K., Douglas, R., Mosca, J. D., Moorman, M. A., Simonetti, D. W., Craig, S., & Marshak, D. R. (1999). Multilineage potential of adult human mesenchymal stem cells. *science*, *284*(5411), 143–147.
- Pont, S. (1987). Thy-1: a lymphoid cell subset marker capable of delivering an activation signal to mouse t lymphocytes. *Biochimie*, *69*(4), 315–320.
- Prockop, D. J. (1997). Marrow stromal cells as stem cells for nonhematopoietic tissues. *Science*, *276*(5309), 71–74.
- Rienecker, K. D., Poston, R. G., & Saha, R. N. (2020). Merits and limitations of studying neuronal depolarization-dependent processes using elevated external potassium. *ASN neuro*, *12*, 1759091420974807.
- Sahu, M., Nikkilä, O., Lågas, S., Kolehmainen, S., & Castrén, E. (2019). Culturing primary neurons from rat hippocampus and cortex. *Neuronal Signaling*, *3*(2). NS20180207.
- Shin, H., Jeong, S., Lee, J.-H., Sun, W., Choi, N., & Cho, I.-J. (2021). 3d high-density microelectrode array with optical stimulation and drug delivery for investigating neural circuit dynamics. *Nature communications*, *12*(1), 492.
- Shin, S. R., Li, Y.-C., Jang, H. L., Khoshakhlagh, P., Akbari, M., Nasajpour, A., Zhang, Y. S., Tamayol, A., & Khademhosseini, A. (2016). Graphene-based materials for tissue engineering. *Advanced drug delivery reviews*, *105*, 255–274.
- Sidney, L. E., Branch, M. J., Dunphy, S. E., Dua, H. S., & Hopkinson, A. (2014). Concise review: evidence for cd34 as a common marker for diverse progenitors. *Stem cells*, *32*(6), 1380–1389.
- Sobacchi, C., Palagano, E., Villa, A., & Menale, C. (2017). Soluble factors on stage to direct mesenchymal stem cells fate. *Frontiers in Bioengineering and Biotechnology*, *5*, 32.
- Stanzione, P. & Tropepi, D. (2011). Drugs and clinical trials in neurodegenerative diseases. *Annali dell'Istituto superiore di sanita*, *47*(1), 49–54.
- Stuart, G., Dodt, H., & Sakmann, B. (1993). Patch-clamp recordings from the soma and dendrites of neurons in brain slices using infrared video microscopy. *Pflügers Archiv*, *423*, 511–518.
- Takahashi, K., Tanabe, K., Ohnuki, M., Narita, M., Ichisaka, T., Tomoda, K., & Yamanaka, S. (2007). Induction of pluripotent stem cells from adult human fibroblasts by defined factors. *cell*, *131*(5), 861–872.
- Tan, K., Zhu, H., Zhang, J., Ouyang, W., Tang, J., Zhang, Y., Qiu, L., Liu, X., Ding, Z., & Deng, X. (2019). Cd73 expression on mesenchymal stem cells dictates the reparative properties via its anti-inflammatory activity. *Stem Cells International*, 2019.
- Tondreau, T., Lagneaux, L., Dejeneffe, M., Delforge, A., Massy, M., Mortier, C., & Bron, D. (2004). Isolation of bm mesenchymal stem cells by plastic adhesion or negative selection: phenotype, proliferation kinetics and differentiation potential. *Cytotherapy*, *6*(4), 372–379.
- Truccolo, W., Donoghue, J. A., Hochberg, L. R., Eskandar, E. N., Madsen, J. R., Anderson, W. S., Brown, E. N., Halgren, E., & Cash, S. S. (2011). Single-neuron dynamics in human focal epilepsy. *Nature neuroscience*, *14*(5), 635–

- Trujillo, C. A., Gao, R., Negraes, P. D., Gu, J., Buchanan, J., Preissl, S., Wang, A., Wu, W., Haddad, G. G., Chaim, I. A., et al. (2019). Complex oscillatory waves emerging from cortical organoids model early human brain network development. *Cell stem cell*, *25*(4), 558–569.
- Urraca, N., Memon, R., El-Iyachi, I., Goorha, S., Valdez, C., Tran, Q. T., Scroggs, R., Miranda-Carboni, G. A., Donaldson, M., Bridges, D., et al. (2015). Characterization of neurons from immortalized dental pulp stem cells for the study of neurogenetic disorders. *Stem cell research*, *15*(3), 722–730.
- Van Dam, D. & De Deyn, P. P. (2011). Animal models in the drug discovery pipeline for alzheimer’s disease. *British journal of pharmacology*, *164*(4), 1285–1300.
- Van Noesel, C., Van Lier, R., Cordell, J., Tse, A., Van Schijndel, G., De Vries, E., Mason, D., & Borst, J. (1991). The membrane igm-associated heterodimer on human b cells is a newly defined b cell antigen that contains the protein product of the mb-1 gene. *Journal of immunology (Baltimore, Md.: 1950)*, *146*(11), 3881–3888.
- Verdi, J., Mortazavi-Tabatabaei, S. A., Sharif, S., Verdi, H., & Shoaee-Hassani, A. (2014). Citalopram increases the differentiation efficacy of bone marrow mesenchymal stem cells into neuronal-like cells. *Neural Regeneration Research*, *9*(8), 845.
- Wang, H.-S., Hung, S.-C., Peng, S.-T., Huang, C.-C., Wei, H.-M., Guo, Y.-J., Fu, Y.-S., Lai, M.-C., & Chen, C.-C. (2004). Mesenchymal stem cells in the wharton’s jelly of the human umbilical cord. *Stem cells*, *22*(7), 1330–1337.
- Wang, K., Wei, G., & Liu, D. (2012). Cd19: a biomarker for b cell development, lymphoma diagnosis and therapy. *Experimental hematology & oncology*, *1*(1), 1–7.
- Wei, C., Liu, Z., Jiang, F., Zeng, B., Huang, M., & Yu, D. (2017). Cellular behaviours of bone marrow-derived mesenchymal stem cells towards pristine graphene oxide nanosheets. *Cell proliferation*, *50*(5), e12367.
- Wilkins, A., Kemp, K., Ginty, M., Hares, K., Mallam, E., & Scolding, N. (2009). Human bone marrow-derived mesenchymal stem cells secrete brain-derived neurotrophic factor which promotes neuronal survival in vitro. *Stem cell research*, *3*(1), 63–70.
- Woodbury, D., Schwarz, E. J., Prockop, D. J., & Black, I. B. (2000). Adult rat and human bone marrow stromal cells differentiate into neurons. *Journal of Neuroscience Research*, *61*(4), 364–370.
- Wu, Y. C., Sonninen, T. M., Peltonen, S., Koistinaho, J., & Lehtonen, Š. (2021). Blood-Brain Barrier and Neurodegenerative Diseases-Modeling with iPSC-Derived Brain Cells. *International journal of molecular sciences*, *22*(14).
- Xicoy, H., Wieringa, B., & Martens, G. J. (2017). The sh-sy5y cell line in parkinson’s disease research: a systematic review. *Molecular neurodegeneration*, *12*, 1–11.
- Yim, E. K., Pang, S. W., & Leong, K. W. (2007). Synthetic nanostructures inducing differentiation of human mesenchymal stem cells into neuronal lineage. *Experimental cell research*, *313*(9), 1820–1829.
- Yu, J., Vodyanik, M. A., Smuga-Otto, K., Antosiewicz-Bourget, J., Frane, J. L., Tian, S., Nie, J., Jonsdottir, G. A., Ruotti, V., Stewart, R., et al. (2007). Induced pluripotent stem cell lines derived from human somatic cells. *science*, *318*(5858), 1917–1920.

- Zakrzewski, W., Dobrzyński, M., Szymonowicz, M., & Rybak, Z. (2019). Stem cells: past, present, and future. *Stem cell research & therapy*, *10*, 1–22.
- Zimmermann, H. (1992). 5'-nucleotidase: molecular structure and functional aspects. *Biochemical Journal*, *285*(Pt 2), 345.

APPENDIX A

```

1
2
3
4
5 % adding multi signal read
6 % calculating real fs by from first signal file
7 % change lowpass filter by band pass filter
8 % change plot original signal and filtered signal
9
10 %%
11 clc;
12 clear;
13 close all;
14 %% Read From File
15 fileID=1681682541;           %Place the name of the first file
16 fileID_top=1681682847;     %Place the name of the last file
17
18 offset_sensor=5;
19 D2v=0.0008056640625; %digital value convert 2 voltage value 3.3v
    /4096=0.0008056640625 volt 3v=Reference VCC 2^12(bit)=4096
20
21
22 k=0;
23 successful_read_file=0;
24 for i=fileID:1:fileID_top
25
26     file_name=sprintf('%d.bin',i);
27     fid=fopen(file_name,'r');
28     if(fid~-=-1)
29         data_byte=fread(fid,'uint16',0,'b');
30         %%% define (size & offset & D2V) sensors
31         SensorSize=((size(data_byte,1)-40)/8)+5 ; %SensorSize
32         if(k==0)
33             Electrode_1=(data_byte(1:(SensorSize*1)-
offset_sensor))*D2v;
34             Electrode_2=(data_byte((SensorSize*1)+1:(
SensorSize*2)-offset_sensor))*D2v;
35             Electrode_3=(data_byte((SensorSize*2)+1:(
SensorSize*3)-offset_sensor))*D2v;
36             Electrode_4=(data_byte((SensorSize*3)+1:(
SensorSize*4)-offset_sensor))*D2v;
37             Electrode_5=(data_byte((SensorSize*4)+1:(
SensorSize*5)-offset_sensor))*D2v;
38             Electrode_6=(data_byte((SensorSize*5)+1:(
SensorSize*6)-offset_sensor))*D2v;
39             Electrode_7=(data_byte((SensorSize*6)+1:(

```

```

SensorSize*7)-offset_sensor))*D2v;
40         Electrode_8=(data_byte((SensorSize*7)+1:(
SensorSize*8)-offset_sensor))*D2v;
41
42
43         else
44             Electrode_1=[Electrode_1;(data_byte(1:(SensorSize
*1)-offset_sensor))*D2v];
45             Electrode_2=[Electrode_2;(data_byte((SensorSize
*1)+1:(SensorSize*2)-offset_sensor))*D2v];
46             Electrode_3=[Electrode_3;(data_byte((SensorSize
*2)+1:(SensorSize*3)-offset_sensor))*D2v];
47             Electrode_4=[Electrode_4;(data_byte((SensorSize
*3)+1:(SensorSize*4)-offset_sensor))*D2v];
48             Electrode_5=[Electrode_5;(data_byte((SensorSize
*4)+1:(SensorSize*5)-offset_sensor))*D2v];
49             Electrode_6=[Electrode_6;(data_byte((SensorSize
*5)+1:(SensorSize*6)-offset_sensor))*D2v];
50             Electrode_7=[Electrode_7;(data_byte((SensorSize
*6)+1:(SensorSize*7)-offset_sensor))*D2v];
51             Electrode_8=[Electrode_8;(data_byte((SensorSize
*7)+1:(SensorSize*8)-offset_sensor))*D2v];
52
53
54         end
55         size(Electrode_1);
56
57 successful_read_file=successful_read_file+1;
58     end
59     k=k+1;
60 end
61 successful_read_file
62
63
64 %% Read Frequency from file
65 file_name=sprintf('%d.bin',fileID);
66 fid=fopen(file_name,'r');
67 value_f=fread(fid,'uint8',0,'b');
68 fclose(fid);
69 time_between_sample= value_f((size(value_f,1)):(size(value_f,1)));
70 time_between_sample
71
72 %% maping data to sensors number
73 %Electrode_1=(data_byte(1:(SensorSize*1)-offset_sensor))*D2v;
74 value=(data_byte(size(data_byte,1)-5:size(data_byte,1)));
75
76

```

```

77 %% define time vector
78 dt=time_between_sample;
79 MXL=(time_between_sample*(size(Electrod_1)-1));%maximun Length
80 t=0:dt:MXL; %define time vector (uS)
81
82
83
84 %%befor down sampling
85 Down_sample_value=1;
86 t_DS=downsample(t,Down_sample_value);
87
88 Electrod_1_DS=downsample(Electrod_1,Down_sample_value);
89 Electrod_2_DS=downsample(Electrod_2,Down_sample_value);
90 Electrod_3_DS=downsample(Electrod_3,Down_sample_value);
91 Electrod_4_DS=downsample(Electrod_4,Down_sample_value);
92 Electrod_5_DS=downsample(Electrod_5,Down_sample_value);
93 Electrod_6_DS=downsample(Electrod_6,Down_sample_value);
94 Electrod_7_DS=downsample(Electrod_7,Down_sample_value);
95 Electrod_8_DS=downsample(Electrod_8,Down_sample_value);
96
97
98 %% define Low pass filter
99 %fp=Pass Frequency
100 %
101
102 %Ap: amount of ripple allowed in the pass band in decibels (the
    default units). Also called Apass.
103 %Ast: attenuation in the stop band in decibels (the default units).
    Also called Astop.
104 %Fp: frequency at the start of the pass band. Specified in
    normalized frequency units. Also called Fpass.
105 %Fst: frequency at the end of the stop band. Specified in
    normalized frequency units. Also called Fstop.
106
107 d = fdesign.bandpass('Fst1,Fp1,Fp2,Fst2,Ast1,Ap,Ast2',1e3,1.1e3,4e3
    ,4.1e3,210,1,210,10e3);
108 HD = design(d,'butter');
109 %% filter signals of sensors by lowpass filter
110 %{
111 Electrod_1_F=filter(HD.Numerator,1,Electrod_1);
112 Electrod_2_F=filter(HD.Numerator,1,Electrod_2);
113 Electrod_3_F=filter(HD.Numerator,1,Electrod_3);
114 Electrod_4_F=filter(HD.Numerator,1,Electrod_4);
115 Electrod_5_F=filter(HD.Numerator,1,Electrod_5);
116 Electrod_6_F=filter(HD.Numerator,1,Electrod_6);
117 Electrod_7_F=filter(HD.Numerator,1,Electrod_7);
118 Electrod_8_F=filter(HD.Numerator,1,Electrod_8);

```

```

119  %}
120
121
122  Electrode_1_DS_F=filter(HD,Electrode_1_DS);
123  Electrode_2_DS_F=filter(HD,Electrode_2_DS);
124  Electrode_3_DS_F=filter(HD,Electrode_3_DS);
125  Electrode_4_DS_F=filter(HD,Electrode_4_DS);
126  Electrode_5_DS_F=filter(HD,Electrode_5_DS);
127  Electrode_6_DS_F=filter(HD,Electrode_6_DS);
128  Electrode_7_DS_F=filter(HD,Electrode_7_DS);
129  Electrode_8_DS_F=filter(HD,Electrode_8_DS);
130
131
132
133  %% after down sampling
134  Down_sample_value=1;
135  t_DS=downsample(t,Down_sample_value);
136
137  Electrode_1_DS=downsample(Electrode_1,Down_sample_value);
138  % Electrode_2_DS=downsample(Electrode_2,Down_sample_value);
139  % Electrode_3_DS=downsample(Electrode_3,Down_sample_value);
140  % Electrode_4_DS=downsample(Electrode_4,Down_sample_value);
141  % Electrode_5_DS=downsample(Electrode_5,Down_sample_value);
142  % Electrode_6_DS=downsample(Electrode_6,Down_sample_value);
143  % Electrode_7_DS=downsample(Electrode_7,Down_sample_value);
144  % Electrode_8_DS=downsample(Electrode_8,Down_sample_value);
145  %
146
147
148
149  %% plot fft original signal and filtered signal
150
151  % x=Electrode_1;
152  % % y = filter(Hd,Electrode_1)
153  % y=Electrode_1_DS_F;
154  %
155  % figure(99) ;
156  %
157  % freq = 0:(2*pi)/length(x):pi;
158  % xdft = fft(x);
159  % ydft = fft(y);
160  % plot(freq,abs(xdft(1:length(x)/2+1)));
161  % hold on;
162  % plot(freq,abs(ydft(1:length(x)/2+1)),'r','linewidth',2);
163  % legend('Original Signal','Bandpass Signal');
164
165  %% plot signals

```

```

166     figure ;
167
168     subplot(4,2,1);
169     plot(t_DS,Electrod_1_DS_F,'R');
170     title('Filtered Electrode #1 ');
171     ylabel('~ volt');
172     axis([0,MXL(1),-0.1,0.1]);
173
174     subplot(4,2,2);
175     plot(t_DS,Electrod_2_DS_F,'R');
176     title('Filtered Electrode #2 ');
177     ylabel('~ volt');
178     axis([0,MXL(1),-0.1,0.1]);
179
180     subplot(4,2,3);
181     plot(t_DS,Electrod_3_DS_F,'R');
182     title('Filtered Electrode #3 ');
183     ylabel('~ volt');
184     axis([0,MXL(1),-0.1,0.1]);
185
186     subplot(4,2,4);
187     plot(t_DS,Electrod_4_DS_F,'R');
188     title('Filtered Electrode #4 ');
189     ylabel('~ volt');
190     axis([0,MXL(1),-0.1,0.1]);
191
192
193     subplot(4,2,5);
194     plot(t_DS,Electrod_5_DS_F,'R');
195     title('Filtered Electrode #5 ');
196     ylabel('~ volt');
197     axis([0,MXL(1),-0.1,0.1]);
198
199     subplot(4,2,6);
200     plot(t_DS,Electrod_6_DS_F,'R');
201     title('Filtered Electrode #6 ');
202     ylabel('~ volt');
203     axis([0,MXL(1),-0.1,0.1]);
204
205     subplot(4,2,7);
206     plot(t_DS,Electrod_7_DS_F,'R');
207     title('Filtered Electrode #7 ');
208     ylabel('~ volt');
209     axis([0,MXL(1),-0.1,0.1]);
210
211     subplot(4,2,8);
212     plot(t_DS,Electrod_8_DS_F,'R');

```

```
213 title('Filtered Electrode #8 ');
214 xlabel('~ time(us)');
215 ylabel('~ volt');
216 axis([0, MXL(1), -0.1, 0.1]);
```